# Edit Trace of Manuscript 10.1021/ci500555g

# Computer -Aided Structure -Based Design of Multitarget Leads for Alzheimer's Disease

**Author, please respond to the following questions:**

Author: Please note that in accordance with ACS style, "ortho" and "meta" have been set in roman rather than italic type when used as adjectives or adverbs (e.g., "ortho substitution", "meta-substituted"). Thanks..... 7

José L. **Domínguez** ,[1†] Fernando **Fernández-Nieto** ,[2‡] Marian **Castro** ,[3§] Marco **Catto** ,[4∥] M. Rita **Paleo** ,[1†,2‡] Silvia **Porto** ,[2‡] F. Javier **Sardina** ,[2‡] José M. **Brea** ,[3§] Angelo **Carotti** ,[4∥] M. Carmen **Villaverde** ,[1†*] **and** Fredy **Sussman** [*1†*]

[1†] **Departamento de Química Orgánica, Facultad de Química**, **Universidad de Santiago de Compostela** , 15782 Santiago de Compostela, Spain.

[2‡] **Centro Singular de Investigación en Química Biológica y Materiales Moleculares (CIQUS)**, **Universidad de Santiago de Compostela** , 15782 Santiago de Compostela, Spain.

[3§] **Departamento de Farmacología, Instituto de Farmacia Industrial, Centro de Investigación en Medicina Molecular y Enfermedades Crónicas (CIMUS)**, **Universidad de Santiago de Compostela** , 15782 Santiago de Compostela, Spain.

[4∥] **Dipartimento di Farmacia-Scienze del Farmaco**, **Università degli Studi di Bari "Aldo Moro"** , 70125 Bari, Italy.

* E-mail: mc.villaverde@usc.es .

*E-mail: fredy.sussman@usc.es.

Alzheimer's disease is a neurodegenerative pathology with unmet clinical needs. A highly desirable approach to this syndrome would be to find a single lead that could bind to some or all of the selected biomolecules that participate in the amyloid cascade, the most accepted route for Alzheimer disease genesis. In order to circumvent the challenge posed by the sizable differences in the binding sites of the molecular targets, we propose a computer -assisted protocol based on a pharmacophore and a set of required interactions with the targets, which that allows for the automated screening of candidates. We used a combination of docking and molecular dynamics protocols in order to discard non-bindersnonbinders, optimize the best candidates, and provide a rationale for their potential as inhibitors. To provide a proof of concept, we proceeded to screen the literature and databases, a task that allowed us to identify a set of carbazole -containing compounds that initially showed affinity only for the cholinergic targets in our experimental assays. Two cycles of design based on our protocol led to a new set of analogues that were synthesized and assayed. The assay results revealed that the designed inhibitors improve their affinityhad improved affinities for BACE-1 by more than three3 orders of magnitude, as well as displaying and also displayed amyloid aggregation inhibition and affinity for AChE and BuChE, a result that led us to a group of multitarget amyloid cascade inhibitors that also could have a positive effect at the cholinergic level.

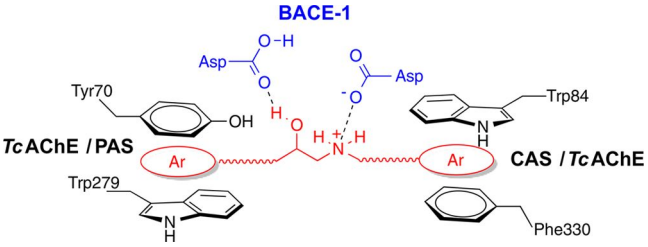


Abstract Graphic

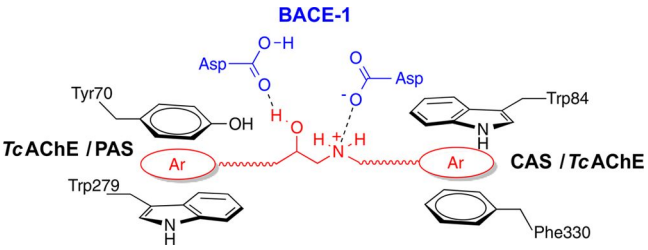


TOC Graphic

SI File: ci500555g_si_001.pdf

## ~~INTRODUCTION~~Introduction

Alzheimer's disease (AD), a cerebral neurodegenerative pathology that is the main cause of dementia in older people, is characterized by the progressive formation of insoluble amyloid plaques and fibrillary tangles. In spite of the enormous efforts carried out by academic institutions and the pharmaceutical industry, AD is an illness with unmet needs since the only drugs available in clinic (i.e., ~~Acetylcholinesterase~~acetylcholinesterase (AChE) inhibitors and ~~a~~an NMDA receptor antagonist) have a palliative effect and do not modify the course of the disease.[1]

The most accepted hypothesis for the origin of AD is the one related to the amyloid cascade, which singles out ~~the~~ aggregates and fibrils of the amyloid peptide (Aβ, a peptide of 40 or 42 residues) as the cause of AD, since their presence interrupts the synaptic connections and precludes the right ~~inter-neuron~~interneuron orientation. [2,3] The ~~Abeta~~Aβ peptides are produced by ~~the~~ hydrolysis of the amyloid precursor protein (APP) by two aspartic proteases (γ-secretase and BACE-1). The ~~last~~past decade has witnessed an all -out effort to discover inhibitors of these two enzymes that could become drug leads for the treatment of AD, but all of the candidates have failed ~~either~~ at ~~pre-clinical~~either preclinical or clinical stages.[3] The inhibition of Aβ peptide aggregation has become an important target for drug lead discovery in itself, although no ~~Abeta~~Aβ aggregation inhibitor has surpassed the clinical assays either.[1] On the other hand, Inestrosa et al.[4] have shown that the peripheral anionic site (PAS) in AChE could be a therapeutic target, since it is a nucleation site for ~~the~~ amyloid ~~Abeta~~Aβ peptide aggregation and hence its inhibition could hinder this process. Finally, ~~the~~ leads that bind AChE~~,~~ could also bind ~~butirylcholinesterase~~butyrylcholinesterase (BuChE~~),~~ and hence have a bearing on the cholinergic pathway by precluding the hydrolysis of acetylcholine and probably enhancing (albeit temporarily) cognition in AD patients.

The multiplicity of amyloid cascade AD targets (described above) opens the door to a new approach ~~towards~~toward single -molecule polypharmacology~~, which~~ that entails the search ~~of~~for a molecule that could bind to all or some of the selected amyloid cascade targets. This novel paradigm, which deviates radically from the one target, one molecule strategy, has recently received increasing attention. [5−7] Probably the major hurdle in the search for multitarget leads ~~lays on~~lies in the substantial structural and specificity differences ~~amongst~~among the binding sites of the amyloid cascade targets, which ~~hinders~~ drastically hinder this therapeutic strategy.[6] These differences are especially noticeable between BACE-1 and the other amyloid cascade targets ~~like~~such as AChE and ~~Abeta peptides~~Aβ peptide aggregation. It has been shown that the compounds aimed at these latter targets share some common traits (~~like~~e.g., the presence of aromatic moieties), an issue that explains the large body of work on this multitarget subset.[7] It would be desirable to find a systematic computer -assisted protocol leading to compounds that bind to the selected set of targets. Herein we postulate the existence of a pharmacophore for a multitarget approach to AD~~, which~~ that bears some of the traits of the ~~know~~known leads that bind a variety of amyloid cascade targets. [5−7] This pharmacophore could be used for a systematic search of novel multitarget leads. As a proof of concept, it has enabled us to identify in the literature some candidates bearing the requirements of our proposed structural framework.[8] Nevertheless, the results of our experimental binding assays indicate that although these compounds bind AChE, they ~~have a~~exhibit modest fibril formation

inhibition and display much lower affinities for BACE-1. Our main endeavor in this work was to generate congeneric ligands with better affinities for all of the amyloid cascade targets selected here. For this sake, we developed a protocol that relies on molecular -docking -based screening for the enzyme targets and molecular dynamics (MD) simulations for peptide aggregation in order to search for more potent analogues of our starting candidates. The main novelty of the protocol elaborated by us is that it allows ~~for~~a systematic search of multitarget leads and their subsequent optimization, given the fact that our hit docking poses should comply with the set of inhibitor~~-~~–protein interactions assigned to our pharmacophore. Review of the predicted docking poses in AChE and BACE-1 revealed possible ways of enhancing binding affinity. Two cycles of design based on our protocol ~~lead~~led to a new set of analogues that were synthesized and assayed. The assay results revealed that the designed inhibitors ~~improve their affinity~~had improved affinities for BACE-1 by more than ~~three~~3 orders of magnitude~~, as well as showing~~ and also displayed affinity for amyloid aggregates, AChE, and BuChE, a result that led us to a group of truly multitarget candidates that interrupt the amyloid cascade while having a positive effect at the cholinergic level.

Furthermore, our results ~~have~~ allowed us to explore some basic questions that relate to molecular recognition issues in the different amyloid cascade targets, including the charge state of the BACE-1 main anchoring group and the mechanism by which the best leads may interrupt the amyloid peptide aggregation.

## Multitarget ~~amyloid cascade pharmacophore~~Amyloid Cascade Pharmacophore

Our pharmacophore was built by identifying the specific moieties that are recognized by the binding pockets of the different amyloid cascade targets. For instance, an essential feature in BACE-1 inhibitors is a functional group (~~such as~~e.g., hydroxyethylene, hydroxyethylamine, guanidium, etc.) ~~which is able to~~that can interact through hydrogen bonds and ion pairs with the Asp dyad, the catalytic machinery of this enzyme.[9] Our choice for this kind of functionality ~~has been~~was based on recent studies in our lab that ~~have~~ identified the hydroxyethylamine group as an Asp dyad anchor ~~which~~that favors good performance at cellular level. [10,11] On the other hand, an overview of the AChE inhibitors ~~indicate~~indicates that many of them contain one or two aromatic moieties ~~which~~that interact through π-stacking interactions with clusters of aromatic residues present ~~both~~ in both the catalytic anionic site (CAS) and ~~in~~ the ~~peripheral binding site (~~PAS~~).~~[12] ~~Both~~The two AChE binding sites are separated by a long gorge. Hence, our ideal AChE inhibitor should include an optimum -length spacer that ~~will connect~~connects the aromatic moiety residing in the CAS with the one at the PAS. If we accomplish this aim, the resulting lead should have both a palliative effect on AD and hinder amyloid aggregation. Finally, some of the amyloid aggregation inhibitors share with the AChE ligands a common feature~~, that is~~namely, the presence of aromatic groups that target some of the residue clusters rich in aromatic residues present in the amyloid peptide (such as the LVFFA segment). Hence, a multitarget pharmacophore and its possible interactions in the amyloid cascade binding sites could be described by a scheme such as the one presented in Figure 1. A number of the features that appear in this pharmacophore have been used in the search ~~of~~for multitarget cascade leads. [5–7] Herein we demonstrate that the ~~pharmacophore~~ described pharmacophore could be used for multitarget screening and subsequent lead optimization.

**Figure 1.** Schematic view of our multitarget pharmacophore (red) bound to the Asp dyad of BACE-1 (blue) and to the CAS and PAS of *Tc*AChE (black).

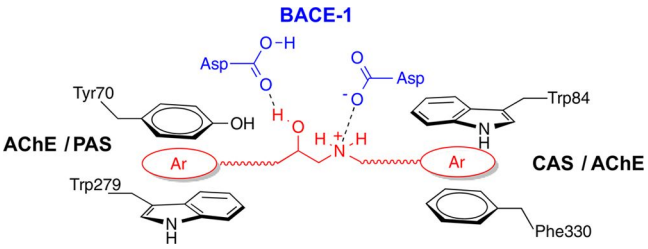


The computer -assisted search for candidates based on the pharmacophore shown in Figure 1 ~~lead~~led us to find some compounds ~~(~~**1**~~)~~ (see Figure 2) with neurogenerative and neuroprotective properties in mice.[8] Nevertheless, the molecular therapeutic targets for these compounds have not been identified. The stated aim of the study that led to these compounds in the first place was to find analogues of dimebon, a carbazole derivative that in itself showed good promise in AD assays in animals but failed in phase ~~three~~-3 clinical trials.[13] Moreover, other carbazole derivatives have been shown to be good ~~Abeta~~Aβ aggregation inhibitors.[14] As ~~seen from~~shown by structure **1** in Figure 2, these

compounds present all of the structural features that make them good leads for all amyloid cascade targets. On one hand the hydroxyethylamine moiety provides an anchor for BACE-1 binding, while the aromatic moieties on both ends (carbazole and substituted phenyl groups) could be a source of affinity of these compounds for AChE and Aβ peptide oligomers. ~~Based on~~On the basis of this information, we decided to investigate ~~if~~whether the original group of compounds ~~(1 )~~ owed ~~its~~their beneficial properties at the ~~CNS~~central nervous system level to their binding to some of the amyloid cascade targets~~,~~ and whether we could produce analogues with better affinity for a wider range of amyloid cascade targets.

**Figure 2.** Structure of dimebon and the analogues ~~(1 )~~ selected for this work.

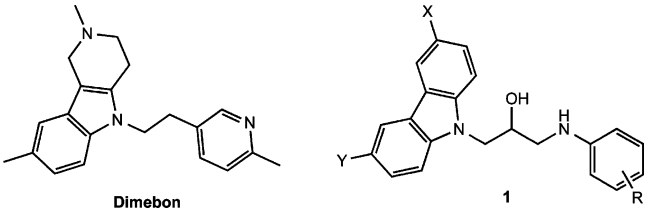


## ~~COMPUTATIONAL METHODS~~Computational Methods

### Pharmacophore ~~based candidate search~~-Based Candidate Search

The quest for compounds bearing the traits of the pharmcophore was performed using the SMILES structure descriptors on bibliographical databases. A variety of different structures were identified, some of them bearing a hydroxyethylamine and others bearing unwanted fragments ~~like~~such as amino ketones. The unwanted candidates were pruned by using a simple AWK script.

### Docking ~~protocols~~Protocols

We carried out the docking simulations with the suite of modules resident in the program GOLD.[15] For each docking run, we employed a minimum of ~~100,000~~100000 and a maximum of ~~1,250,000~~1250000 genetic generated poses. We scored the poses with three of the scoring functions resident in GOLD (i.e., GoldScore, [16,17] ChemScore, [18–20] and ChemPLP[21] ).

### Docking to BACE-1

One of the most outstanding structural features of the active site of BACE-1 is a residue segment (residues 69−75) that forms a flap ~~(residues 69 to 75)~~ whose conformational variability allows for a great variety of binding poses for those inhibitors differing in size and shape.[9] This loop, which forms part of the S1 pocket, closes in ~~onto~~on the active site during substrate catalysis. There are inhibitors that bind explicitly to the flap ~~avoiding~~, preventing its closure and hence hampering catalysis. Perusal of the many BACE-~~1~~– inhibitor complex structures indicates that the flap presents a wide variety of openings depending on the inhibitor's chemical nature. In order to take ~~into account~~ the flap variability into account in our docking calculations, we ~~have~~ carried out our docking simulations with three protein templates that differ in the opening of this loop. The first of these protein structures comes from the complex between BACE-1 and the peptide-mimetic inhibitor **OM99-2** (PDB entry ~~1FKN~~1FKN ) and has a closed flap.[22] The second structure has a non-peptidic inhibitor bound to the enzyme with a middle -range opening of the flap (PDB entry ~~3KMY~~3KMY ),[23] while the last template was obtained from the unbound structure of BACE-~~1~~, and has a fully opened flap (PDB entry ~~1W50~~1W50 ).[24] Figure 3 ~~exhibits the~~shows a superposition of these three structures with the flap structures displayed in different colors.

~~Our previous studies, which combined SPR binding experiments with molecular mechanics based calculations, predicted that the Asp dyad in BACE-1 has a monoprotonated state (at pH values ranging from 4.5 to 7.4) when bound to compounds with a hydroxyethylamine moiety.[10] Thus, we assigned this Asp dyad state to BACE-1 in our docking screening calculations. On the other hand, the aniline present in our compounds could be protonated or neutral at the acidic pH (4.5-5.0) at which the experimental assays are carried out. For this reason docking simulations for these compounds were carried out both with neutral and protonated anilines.~~

~~As a first step we cleaned up the target structures mentioned above, eliminating the crystallographic water molecules, discarding alternative conformations and adding hydrogen atoms, by using the Discovery Studio (DS) modules.[25] We defined the targeted binding site for GOLD docking to these proteins as all the atom residues that were within 6Å of the inhibitor in the 3KMY complex.~~

**Figure 3.** Superimposition of ~~1FKN~~the 1FKN , ~~3KMY~~3KMY , and ~~1W50~~1W50 protein ribbon structures. The flap loops are colored in green, blue, and red, respectively.

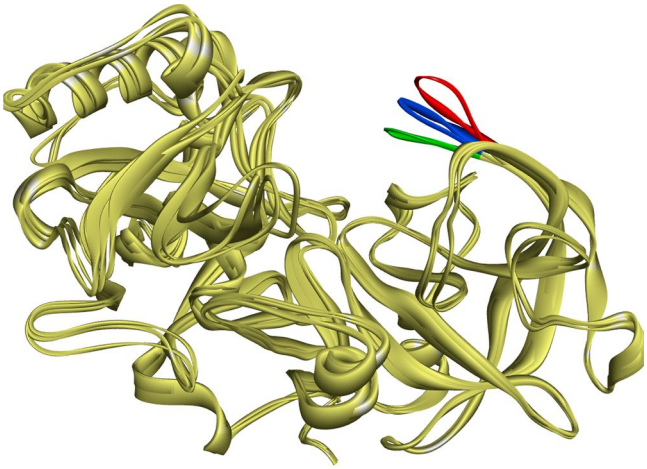

Our previous studies, which combined surface plasmon resonance binding experiments with molecular-mechanics-based calculations, predicted that the Asp dyad in BACE-1 has a monoprotonated state (at pH values ranging from 4.5 to 7.4) when bound to compounds with a hydroxyethylamine moiety.[10] Thus, we assigned this Asp dyad state to BACE-1 in our docking screening calculations. On the other hand, the aniline present in our compounds could be protonated or neutral at the acidic pH (4.5−5.0) at which the experimental assays were carried out. For this reason, docking simulations for these compounds were carried out both with neutral and protonated anilines.

As a first step, we cleaned up the target structures mentioned above by eliminating the crystallographic water molecules, discarding alternative conformations, and adding hydrogen atoms using the Discovery Studio (DS) modules.[25] We defined the targeted binding site for GOLD docking to these proteins as all of the atom residues within 6 Å of the inhibitor in the 3KMY complex.

For each of the structures differing in the flap opening, we then performed docking calculations with one of the three scoring functions (ChemScore, ~~GoldSCore~~GoldScore, and ChemPLP). In each of the runs, we searched for the presence of a single hit pose ~~amongst~~among the top ~~ten docking~~10 resulting docking poses. We ~~define~~defined a hit pose as ~~the~~ one that ~~will fulfill~~fulfills the hydrogen ~~bond~~-bonding pattern between the hydroxyethylamine fragment and the Asp dyad shown for our pharmacophore in Figure 1. Global success rates for every ~~compound~~ candidate compound were calculated by adding up the ~~number~~numbers of single hits of the docking simulations carried out with the three scoring functions for our three protein templates differing in the flap opening described above.

Docking to AChE

For the docking predictions to this target, we used the X-ray structure of *Torpedo californica* ~~Torpedo californica~~ (*Tc*AChE) complexed with a bis-(tacrine) analogue (PDB entry ~~1ODC~~1ODC ).[26] A close -up of the binding pose is shown in Figure 4. In the same way as for BACE-1, we cleaned up the target structure (PDB entry 1ODC ) by eliminating the crystallographic water molecules, discarding alternative conformations, and adding hydrogen atoms using the DS modules.[25] We defined the binding site as all of the AChE atom residues that lay at 6 Å from the ligand of this complex (i.e., the bis(tacrine) analogue). Again, the docking conformations generated by the genetic algorithm were evaluated using the same scoring functions as for BACE-1. In each run, the top 10 poses were screened for compliance with the face-to-face π-stacking interactions that optimize the inhibitor affinity at both the CAS and PAS in AChE, as shown in Figure 1 and exemplified by the bis(tacrine) analogue in Figure 4 . In the same way as in BACE-1, the hit success rate was determined by searching for a hit among the top 10 poses for the docking simulations evaluated with our three scoring functions. Global success rates were calculated by adding up the numbers of single hits.

**Figure 4.** Close -up ~~to~~of the binding of the indicated bis-(tacrine) analogue ~~indicated~~ to both binding sites (CAS and PAS) in *Tc*AChE (from PDB entry ~~1ODC~~1ODC ). The inhibitor is shown in blue, and the aromatic residues are shown

in green. ~~Notice the~~The π – π interactions ~~between~~of the aromatic moieties ~~and~~with the side chains of residues Trp 84 and Phe 330 at the CAS and with residues Tyr 70 and Trp 279 at the PAS should be noted.

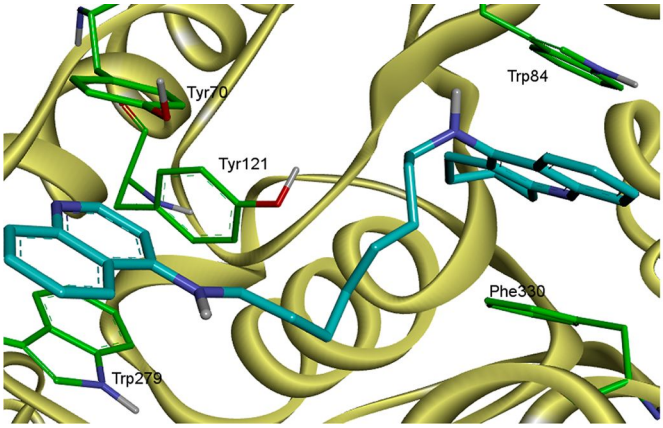



~~In the same way as for BACE-1, we cleaned up the target structure (PDB id 1ODC), eliminating the crystallographic water molecules, discarding alternative conformations and adding hydrogen atoms, by using the Discovery Studio (DS) modules.[25] We defined the binding site as all the AChE atom residues that lay at 6 Å from the ligand of this complex (i.e., the bis-tacrine analogue). Again, the docking conformations generated by the genetic algorithm were evaluated by the same scoring functions used for BACE-1. In each run the top ten poses were screened for compliance with the face-to-face π-stacking interactions that will optimize the inhibitor affinity both at the CAS and PAS in AChE, as shown in Figure 1 and exemplified by the bis-tacrine analogue in Figure 4. In the same way as in BACE-1 the hit success rate was determined by searching for a hit amongst the top ten poses for the docking simulations evaluated with our three scoring functions. Global success rates were calculated by adding up the number of single hits.~~

## Aβ ~~aggregation inhibition protocol~~Aggregation Inhibition Protocol

As we explained in the ~~introduction~~Introduction , one of the therapeutic targets is ~~the~~ inhibition of the Aβ peptide oligomerization that leads to the neuronal toxic species. These peptides do not have a unique binding site for the ligands as in the case of other AD amyloid cascade enzymatic targets. Depending on the nature of the ligand, there are multiple binding sites that share similar sequence motifs. For instance, some aromatic moiety inhibitors tend to bind to aromatic residue clusters present in the LVFFA segment of the amyloid peptide.[27] Hence, many in silico aggregation inhibition studies merge docking protocols with ~~molecular dynamics (~~MD~~)~~ simulations.[28] We ~~have~~ explored a different approach recently developed by the group of Caflisch.[27a] It consists ~~in~~of analyzing lengthy MD simulations of a segment of the Aβ peptide (Aβ12–28) in the presence of a given candidate. This peptide fragment ~~has been~~was chosen for several reasons. ~~Firstly~~First, the first 11 residues were omitted since they lack any definite secondary structure in some NMR amyloid aggregate structures.[29] Moreover, the selected segment contains one of the regions (LVFFA) around which a ~~beta~~ β-hairpin~~,~~ (the template for ~~Abeta~~Aβ aggregation) forms~~,~~ and is also one of the ligand's binding spots for a number of ligands.[27] Finally, this segment has been used in NMR -based experiments to study ligand binding locations.[27b]

Our extensive MD calculations were carried out with the CHARMM PARAM-19 force field,[30] which employs an extended atom approximation for all carbon atoms. Protonation states of all titratable residues were considered at neutral pH. In particular, the side chains of the His residues were assigned a neutral charge, whereas the basic residues (Arg/Lys) and the acidic residues (Asp/Glu) were assigned ~~either a~~ positive ~~or a~~and negative ~~charge~~charges, respectively. We used an implicit solvation protocol called ~~FACTS (Fast Analytical Continuum Treatment~~fast analytical continuum treatment of ~~Solvent~~solvent (FACTS), an efficient generalized Born (GB) implicit solvation model developed ~~in~~by Caflisch's group,[31] which includes a solvent -accessible surface of the solute for the ~~non-polar~~nonpolar contribution.

MD ~~Simulations~~simulations were carried out with periodic boundary conditions at a fixed peptide concentration of 2.5 mM (87 ~~Å~~Å cubic simulation box) using the Langevin integrator at low friction (coefficient of 0.15 $ps^{-1}$) and ~~at~~ a temperature of 300 K. Using a time step of 2 fs, for each system~~,~~ we performed five independent runs ~~which~~that added up to a 5 μs trajectory. Each of the starting structures contained the peptide in an extended conformation to-

gether with the inhibitor candidate in a different position. ~~We also used as~~As a reference ~~the~~, we used simulations of a peptide with the known aggregation inhibitor 9,10- anthraquinone and of the ligand-free peptide. The initial structures were subjected to two energy minimization runs, which began ~~by~~with a 500 ~~steps~~-step steepest descent run followed by a ~~50,000 steps~~50000-step conjugate gradient calculation. In each case, the gradient tolerance was ~~of~~ 0.001 ~~kcal/(mol·Å~~kcal·mol$^{-1}$·Å$^{-2}$~~)~~. Then~~,~~ a 0.5 ns heating stage and a 0.5 ns thermal MD equilibration ~~stages spanning 0.5 ns each~~stage were carried out, followed by the production stage described above.

Since every MD simulation ~~takes a~~took 1 month of wall ~~-~~clock computer time, we had to select the kind and number of compounds used in our calculations. For instance, for the indole derivatives we performed simulations ~~only~~ on only one aniline~~-~~ and two benzylamine ~~-~~containing compounds (see below). Our simulations were then used to calculate the average ~~residency time~~residence times of the ligand around the peptide and around every residue of the peptide~~,~~ as well as the effect of the ligand on the secondary structure of the peptide. The statistical significance of these results is provided by the standard deviations based on the individual trajectories.

## ~~RESULTS~~Results

### 1. First ~~lead optimization~~Lead Optimization: Carbazole ~~derivatives~~Derivatives

**1.1.** BACE-1 ~~ligand screening~~Ligand Screening. The first set of compounds studied were the carbazole derivatives bearing an aniline moiety with a substituent at either ~~in~~the ortho or meta ~~positions,~~position that originally showed neuroprotective and neurogenerative activity in mice.[8] From this study we chose a subset whose chemical structures and docking ~~results~~ data are displayed in Table S1 in the ~~supporting info~~Supporting Information, while the global docking success rates (see ~~methods~~Computational Methods ~~section~~ for details) are shown in Figure 5. As can be seen from Figure 5 and Table S1, the compounds that have a methoxy substituent ~~at~~on the aniline at either ~~in~~ the ortho position (compound **1d**) ~~and at~~or the meta position (compound **1g**) are the ones that show the widest consensus as ~~a~~ possible BACE-1 ~~inhibitor~~inhibitors. The better fit displayed by these compounds could be the result of reduced steric clashes, ~~given that~~as they are the smallest candidates in this list. For the same reason, our predictions indicate that the smaller ligands bind to BACE-1 with any of the three flap openings (see Table S1). Nevertheless, given their size, it is doubtful that these ligands could span both the CAS and PAS in AChE~~,~~ and hence become multitarget leads.

**Author: Please note that in accordance with ACS style, “ortho” and “meta” have been set in roman rather than italic type when used as adjectives or adverbs (e.g., “ortho substitution”, “meta-substituted”). Thanks.**

~~Perusal of the results in Figure 5 and Table S1 shows that the available hits are obtained almost exclusively when the docking calculations are carried out with a charged ligand. Actually, only two of the seven compounds (**1e, 1g**) display some hits when neutral. This result is in line with our previous studies,[32] which indicate that there is an enrichment in the number of predicted poses close to those observed experimentally when the ligand is charged.~~

**Figure 5.** Global BACE-1 docking success rates ~~for BACE~~of aniline ~~-1~~substitued ligands as provided by the ~~number~~numbers of single hits across flap openings and docking scoring functions. Neut and Prot indicate ~~weather the ligand is~~ neutral ~~or~~and protonated ligands, respectively.

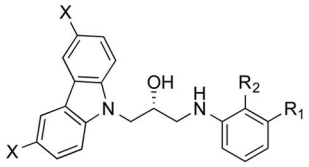


**1a**: X = H, $R_1$ = H, $R_2$ = OMe
**1b**: X = H, $R_1$ = H, $R_2$ = OBn
**1c**: X = H, $R_1$ = H, $R_2$ = $OCH_2CH_2Ph$
**1d**: X = Br, $R_1$ = H, $R_2$ = OMe
**1e**: X = Br, $R_1$ = H, $R_2$ = OBn
**1f**: X = Br, $R_1$ = H, $R_2$ = $OCH_2CH_2Ph$
**1g**: X = Br, $R_1$ = OMe, $R_2$ = H

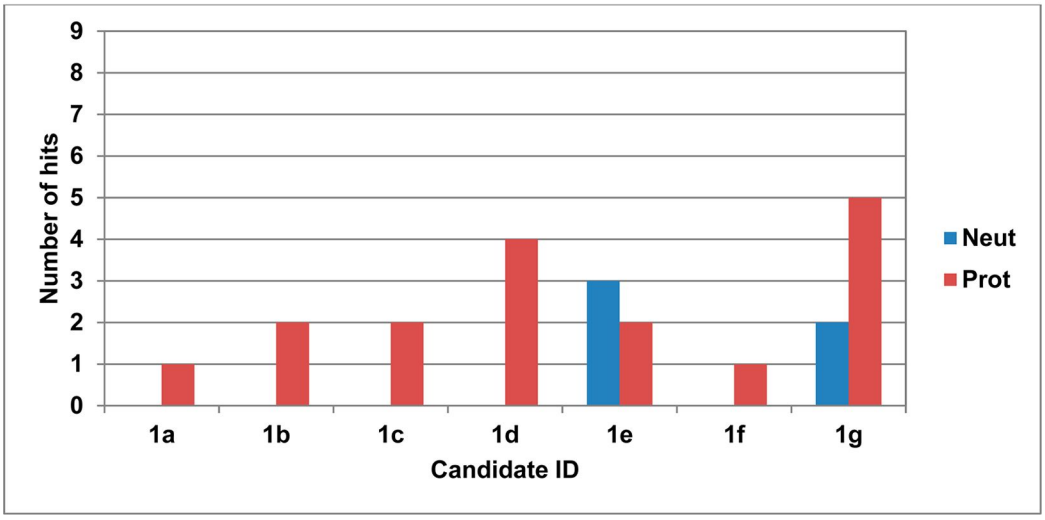


Perusal of the results in Figure 5 and Table S1 shows that the available hits were obtained almost exclusively when the docking calculations were carried out with a charged ligand. Actually, only two of the seven compounds (**1e** and **1g**) displayed some hits when neutral. This result is in line with our previous studies,[32] which indicate that there is an enrichment in the number of predicted poses close to those observed experimentally when the ligand is charged.

The p$K_a$ of the protonated amino group belonging to the aniline moiety, for these compounds in solution, is ca. 4.7, a value that is close to the pH at which the binding assays were performed. Replacing the aniline by a benzylamine moiety was expected to increase the p$K_a$ of the amino group and hence the likelihood that it would be charged, an outcome that should boost the number of predicted BACE-1 binders. Figure 6 displays the global hit success for benzylamine -containing compounds substituted at the ortho position (upper panel) or the meta position (lower panel). The detailed data for these docking calculations are shown in Tables S2 and S3. Comparison of the numbers of single hits among the top 10 exit poses for analogous aniline (Table S1 and Figure 5) and benzylamine compounds (Tables S2 and S3 and Figure 6), compounds indicates a substantial increase in the hit rates for benzylamines above those calculated for the aniline -containing compounds, an outcome that validates our design premises.

**Figure 6.** Global hit success resulting from the docking to BACE-1 of (top) protonated ortho-substituted benzylamines and (bottom) both neutral and protonated meta-substituted benzylamines. R and S indicate the two possible enantiomeric configurations of each compound.

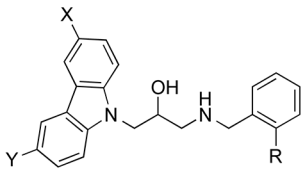


**2a**: X = Y = H, R = OMe
**2b**: X = Y = H, R = OBn
**2c**: X = Y = H, R = $OCH_2CH_2Ph$
**2d**: X = Y = Br, R = OMe
**2e**: X = Y = Br, R = OBn
**2f**: X = Y = Br, R = $OCH_2CH_2Ph$
**2g**: X = Br, Y = Me, R = OBn
**2h**: X = Br, Y = Me, R = $OCH_2CH_2Ph$

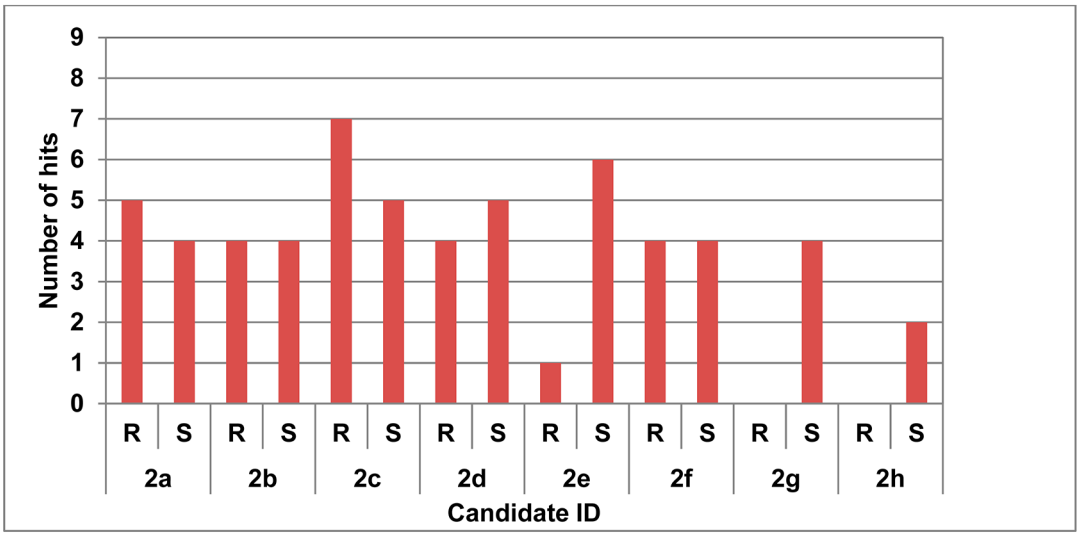


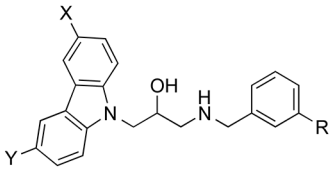


**3a**: X = Y = H, R = OMe
**3b**: X = Y = H, R = OBn
**3c**: X = Y = H, R = $OCH_2CH_2Ph$
**3d**: X = Y = Br, R = OMe
**3e**: X = Y = Br, R = OBn
**3f**: X = Y = Br, R = $OCH_2CH_2Ph$
**3g**: X = Br, Y = Me, R = OBn
**3h**: X = Br, Y = Me, R = $OCH_2CH_2Ph$

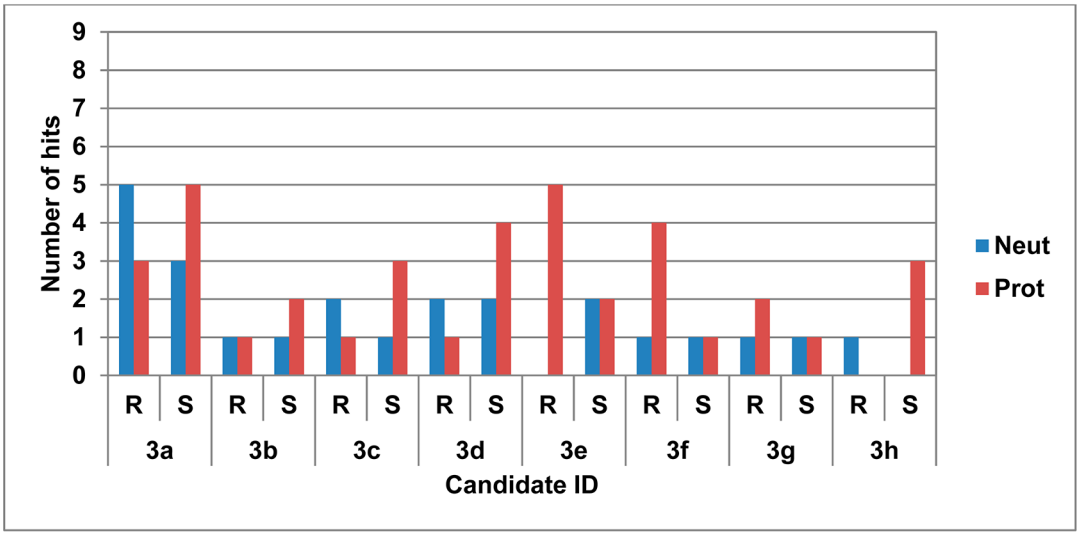

Perusal of Figure 6 indicates that the benzylamine substitution pattern ~~has~~ also has a bearing ~~in~~on the number of possible hits. The results would seem to indicate that ~~the~~ortho ~~ortho~~substitution is favored over ~~the~~ meta substitution ~~at~~on the benzylamine moiety. For instance ~~amongst~~, among the top ~~ten~~10 poses, the number of single hits with ortho substitution is twice the number of hits with ~~the~~ meta substitution (see Tables S2 and S3). Nevertheless, there ~~seems~~seem to be exceptions (e.g., see ~~compounds~~compound **3e** when the hydroxyl group is in the *R* configuration~~),~~ ~~which~~ that had ~~a number~~numbers of hits comparable to those for the analogous ortho ~~derivative~~derivatives ~~(i.e~~e.g., compound **2e** when the hydroxyl group is in the *S* configuration).

For the compounds bearing a benzylamine fragment we also analyzed the effectiveness of each stereoisomer. The results ~~shown~~presented in Figure 6 do not show a clear predilection for a given enantiomer, as changes at the end points of the candidate compounds seem to change the preference. For instance, in the case of the compounds containing meta-substituted benzylamines, those compounds ~~that bear~~bearing two Br atoms on the carbazole favor ~~a~~the *R* configuration (compounds **3e** and **3f**), while those ~~that replace~~with both Br atoms replaced by H atoms favor ~~a~~the *S* configuration. Nevertheless, these configuration patterns do not seem to hold for the ortho-substituted benzylamine -bearing compounds.

**1.2.** AChE ~~ligand screening~~Ligand Screening. Figure 7 displays the AChE global hit ~~rate~~rates for protonated anilines and benzylamines ~~(~~substituted ~~in~~at the ortho position~~),~~ while Figure 8 depicts the ~~number~~numbers of hits for the compounds bearing ~~benzylamines~~ meta-substituted ~~in~~ benzylamines*~~meta~~*. As ~~seen from~~ these figures show, there is a wide consensus ~~amongst~~among the scoring function results, indicating that these compounds are good candidates for AChE inhibitors, in most cases independently of the stereochemistry of the hydroxyl group and the charge of the ~~hydroxylethylamino~~hydroxyethylamino group. Comparison with the BACE-1 docking results described above indicates that the ~~number~~numbers of predicted hits for AChE ~~is~~are substantially larger than those for BACE-1, implying that there are fewer hurdles for finding a candidate that will fulfill the pharmacophore requirements for the former enzyme.

**Figure 7.** Global hit ~~rate~~rates resulting from the AChE docking screening of the protonated ortho -substituted anilines (left) and benzylamines (right). The hit search was carried ~~amongst~~out among the top ~~ten~~10 poses resulting from three docking calculations, each carried out with a different scoring function (ChemScore, GoldScore ~~and~~, or ChemPLP).

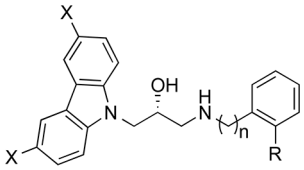


**1a**: X = H, n = 0, R = OMe
**1b**: X = H, n = 0, R = OBn
**1c**: X = H, n = 0, R = $OCH_2CH_2Ph$
**1d**: X = Br, n = 0, R = OMe
**1e**: X = Br, n = 0, R = OBn
**1f**: X = Br, n = 0, R = $OCH_2CH_2Ph$

**2a**: X = H, n = 1, R = OMe
**2b**: X = H, n = 1, R = OBn
**2c**: X = H, n = 1, R = $OCH_2CH_2Ph$
**2d**: X = Br, n = 1, R = OMe
**2e**: X = Br, n = 1, R = OBn
**2f**: X = Br, n = 1, R = $OCH_2CH_2Ph$

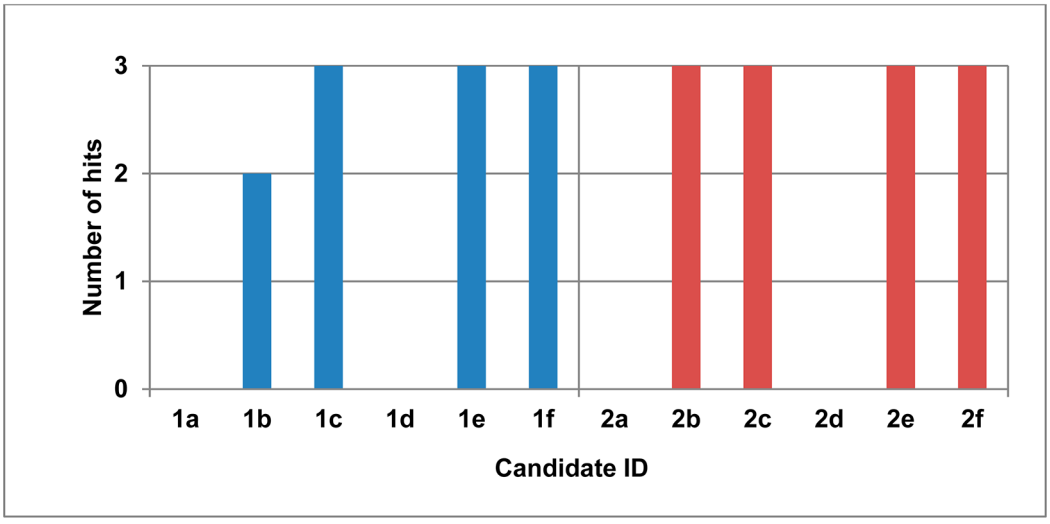


**Figure 8.** Global hit ~~rate~~rates resulting from the AChE docking screening of the compounds with a meta -substituted benzylamine. For each molecule, we studied the effect of the stereochemistry of the hydroxyl group (*R*~~,~~ or *S*) and

the protonation state of the amine ~~group. The~~group. The hit search was carried ~~amongst~~out among the top ~~ten~~10 poses resulting from three docking calculations, each carried out with a different scoring function (ChemScore, GoldScore ~~and~~, or ChemPLP).

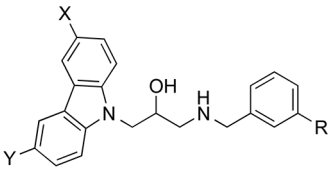


**3b**: X = Y = H, R = OBn
**3c**: X = Y = H, R = $OCH_2CH_2Ph$
**3e**: X = Y = Br, R = OBn
**3f**: X = Y = Br, R = $OCH_2CH_2Ph$
**3g**: X = Br, Y = Me, R = OBn
**3h**: X = Br, Y = Me, R = $OCH_2CH_2Ph$

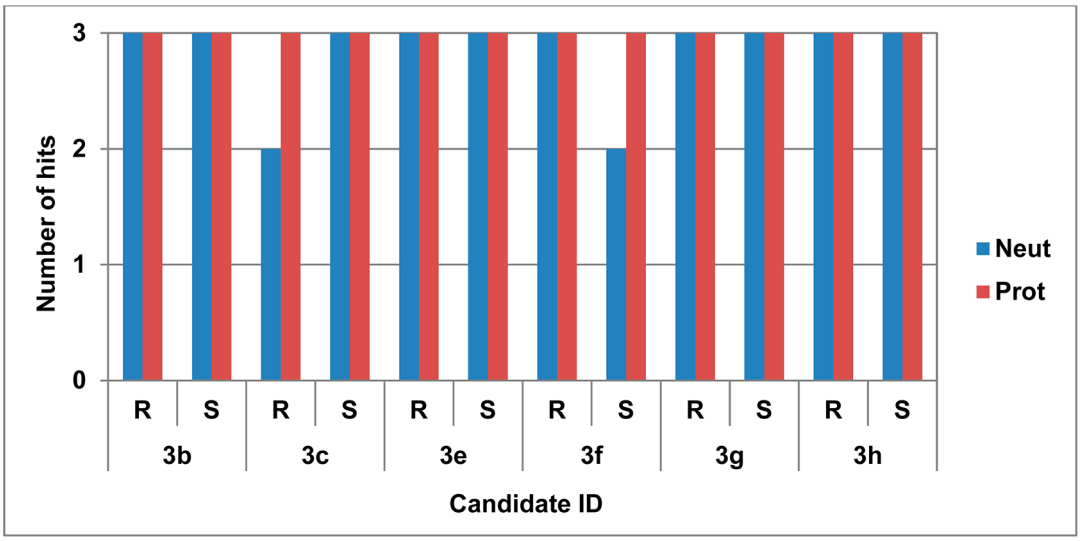


The scoring function values for aniline- and benzylamine -containing compounds are listed in Tables S4 and S5. Perusal of Table S4 and Figure 7 indicates that the shorter compounds, ~~like~~such as **1a**, **1d**, **2a** and **2d** (those bearing a methoxy substituent), have no ~~hit~~hits according to our pharmacophore definition~~, as~~ shown in Figure 1. Scrutiny of the binding ~~poses~~pose for a methoxy ~~as~~-substituted compound compared ~~to~~with that for a benzyloxy -substituted compound (Figure 9) indicates that the former ligands derive their worse performance from their inability to bind ~~both~~ to both the CAS and PAS in AChE. As ~~seen from~~shown in Figure 9 , the carbazole moiety interacts ~~in the CAS~~ with residues Tyr 84 and Phe 330 in the CAS through π -stacking interactions. The shorter ligand is not able to reach the PAS in AChE and hence ~~to~~cannot generate these types of interactions with Tyr 70 and Trp 279.

**Figure 9.** Docking of compounds **2d** (~~upper panel~~top) and **3b** (~~lower panel~~bottom) into AChE.

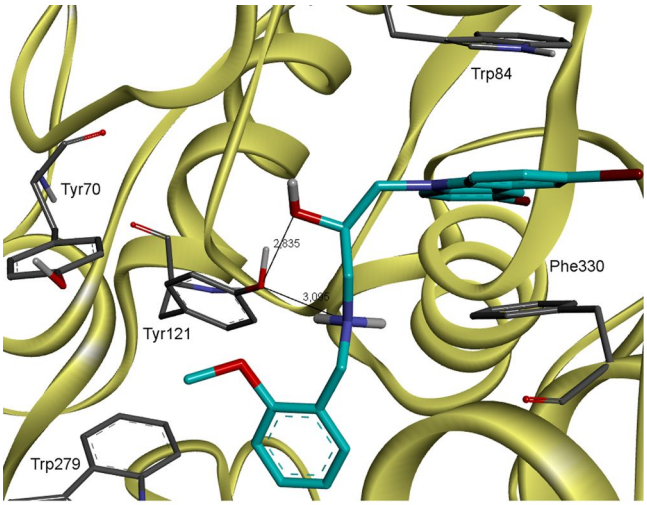


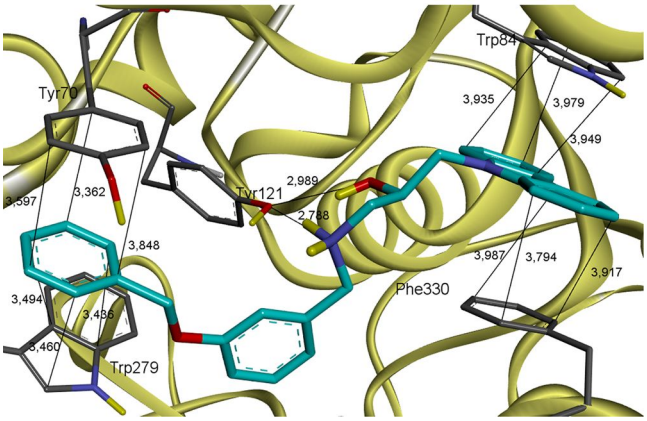


**1.3.** ~~Inhibitor~~ Aβ12~~–~~–28 ~~peptide interaction results~~Peptide Interaction Inhibition Results. Table 1 lists the percentage ~~of~~ residence times for 9,10-anthraquinone (a reference compound) and for some carbazole -containing compounds~~,~~ up to 7.5 ~~Å~~Å from the peptide. We ~~have~~ also calculated the residence ~~time~~times of these ligands around every residue of the peptide with a ~~cut off~~cutoff distance of 4.5 ~~Å~~Å (see Figure 10) and the residue~~–~~–residue ~~interaction~~interactions in the absence ~~and~~or presence of the ligands (see ~~Figures~~Figure 11 and Figure S4 in the ~~S4~~Supporting Information). As ~~seen from~~shown in Table 1, the candidate compounds have ~~a~~ much larger residence ~~time~~times than the reference ligand. Moreover, the selected compounds display a bigger preference (~~than~~compared with the reference compound) for the binding hot spots centered on both the His cluster at the N -terminal end and ~~on~~ the aromatic cluster found at the LVFFA segment.

**Table 1.** Percentage ~~of residence time~~Residence Times for ~~contacts peptide–ligand~~Peptide−Ligand Contacts up to 7.5 ~~Å~~Å

| ~~Candidate~~candidate | ~~Contact Time (~~contact time $^{K}$(%)$^{T}$ ~~%)~~ |
|---|---|
| **1a** | ~~85$^{K}$~~85 ± 2.6$^{T}$ ~~± 2.6~~ |
| **1b** | ~~93$^{K}$~~93 ± 0.6$^{T}$ ~~± 0.6~~ |
| **1c** | ~~90$^{K}$~~90 ± 2.0$^{T}$ ~~± 2.0~~ |

| Candidatecandidate | Contact Time (contact time K(%)T %) |
|---|---|
| **1d** | 99K99 ± 0.4T ± 0.4 |
| **1f** | 99K99 ± 0.2T ± 0.2 |
| anthraquinone | 36K36 ± 1.5T ± 1.5 |

**Figure 10.** Ligand – peptide residues fractionresidue contact timestime fractions. Cut offThe cutoff distance iswas set at 4.5 ÅÅ.

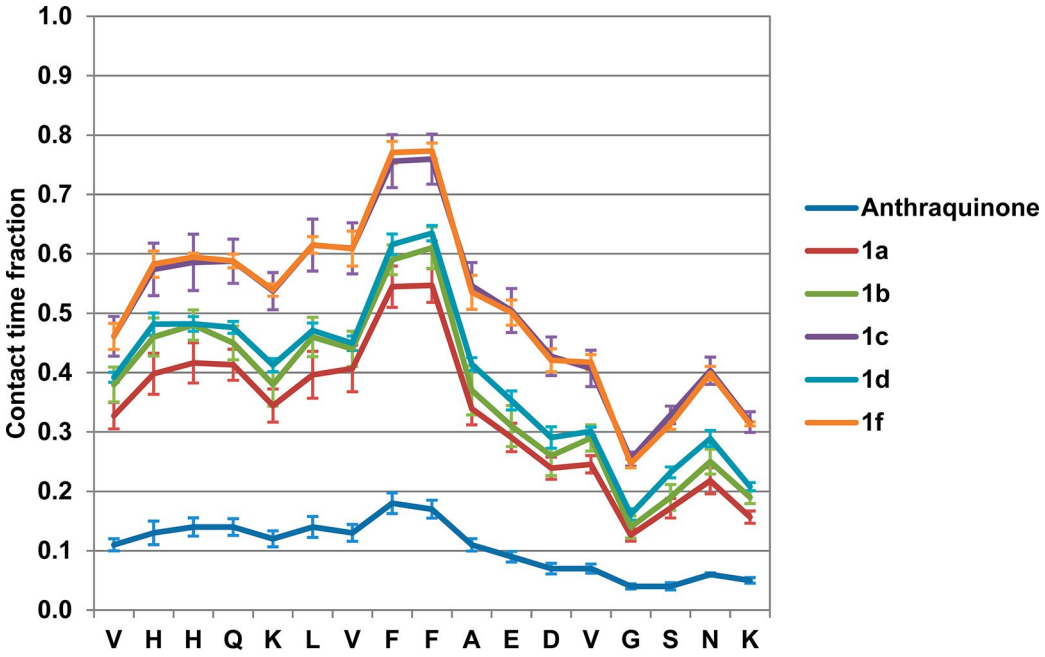


**Figure 11.** Residue – residue contact mapmaps in the absence (top -left panel) and in theor presence of inhibitors. Cut offThe cutoff interaction distance iswas set at 4.5 ÅÅ. The color scale shown aboveat the bottom indicates the fraction residence timestime fractions.

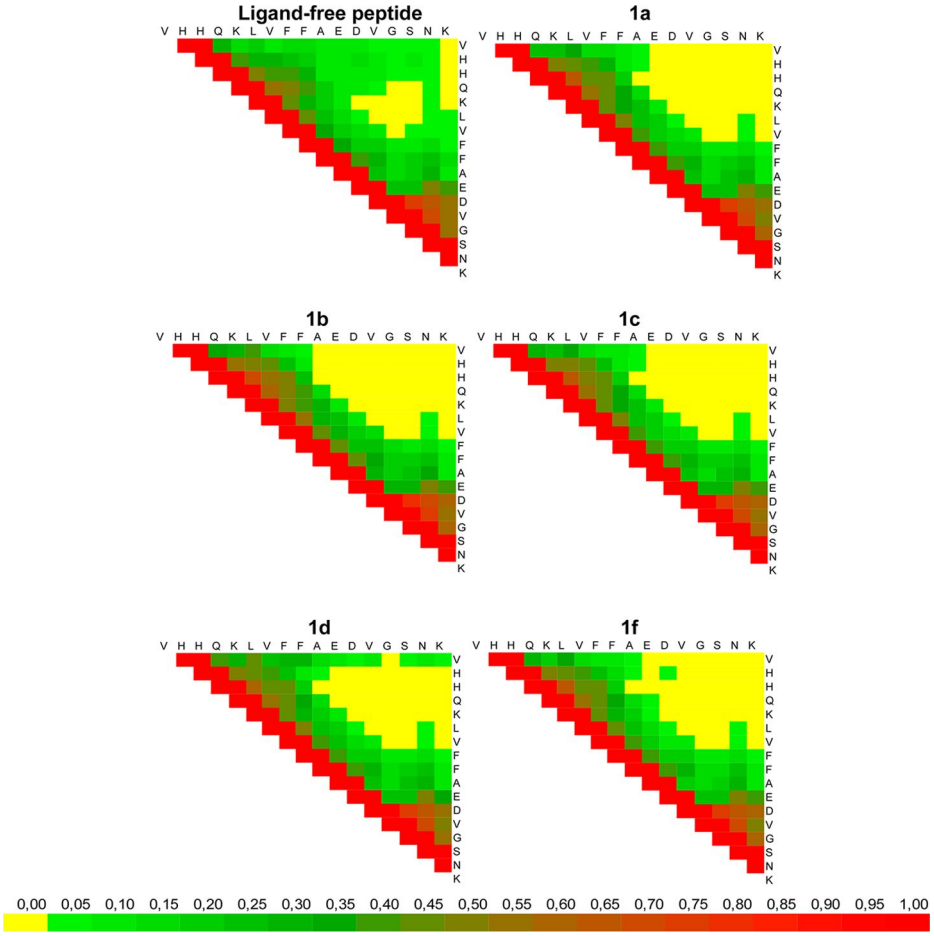


An important issue is the effect of the ligand on the secondary structure of the peptide. The Aβ peptide, which originates from APP hydrolysis, originally adopts a helix structure. As amyloid aggregates are formed, there is a change of conformation that leads to a ~~beta~~ β-hairpin, specifically around the DVGS motif. For instance, the NMR structure of a pentamer[29] ~~shows~~ clearly shows that the peptides organize themselves ~~forming~~to form hairpins that aggregate as sheets. As ~~seen from~~shown in Figures 11 ~~an~~and S4, the ligands would seem to partially preclude the formation of this secondary structure motif (turn) in a monomer, a process that may lead to ~~a~~ reduced aggregation. Hence, it may be surmised that the residue–residue contact map in the presence of a ligand may give us a measure of the ~~inhibitory~~ aggregation inhibition effect of our candidates.

**1.4.** Synthesis and ~~experimental assays~~Experimental Assays for ~~carbazole containing compounds~~Carbazole-Containing Compounds. The synthesis of several carbazole-containing compounds was carried out following Scheme 1, which includes the list of synthesized molecules. Carbazole~~epoxide~~ epoxides **10** ~~was~~were prepared as described in the literature from ~~carbazole (~~carbazoles **8** ~~)~~ and epichlorohydrin (**9** ). [8,33] Regioselective ring-opening of ~~epoxide~~epoxides **10** with different ortho-substituted anilines **11** in the presence of $Mg(ClO_4)_2$ in acetonitrile,[34] afforded carbazole compounds **1** in moderate to good yields. Similarly, as shown in Scheme 1, carbazole analogues **3** were synthesized by ring opening of carbazole~~epoxide~~ epoxides **10** with meta-substituted benzylamines **12**. The choice of compounds was guided in many cases by the availability of the reactants. Although in the case of benzylamines the compounds with an ortho substituent ~~seem~~seemed to show a wider consensus as BACE-1 inhibitors across all of the scoring functions (see Figure 6), they require ~~a~~ more ~~elaborated~~elaborate and expensive chemistry. For this reason, we chose the best -scoring candidates with a meta -substituted benzylamine (**3e** and **3f**).

**Scheme 1.** Synthetic ~~route~~Routes and ~~carbazole derivatives synthesized.~~Carbazole Derivatives Synthesized

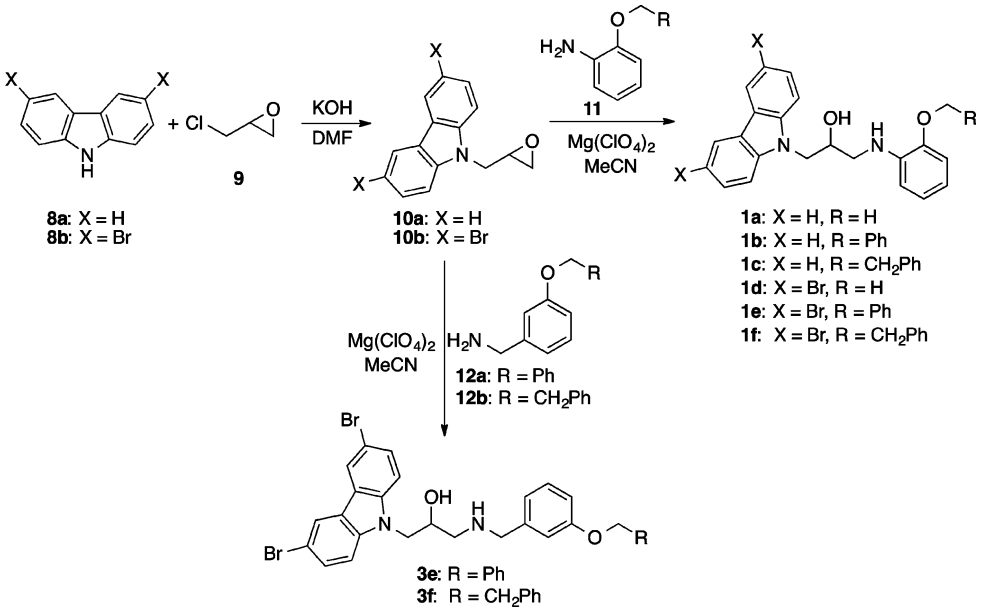


The results ~~for~~of the experimental binding assays ~~in~~with BACE-1, AChE, and BuChE~~,~~ as well as the ThT Aβ aggregation inhibition assays are shown in Table 2. As ~~seen from~~shown in this table, some of the aniline-containing compounds ~~showed some~~demonstrated promise as multitarget inhibitors. For instance, compounds **1e** and **1f** ~~display μM~~displayed micromolar binding affinity for AChE and Aβ inhibition ~~percentage~~percentages of ca. 50% at 100 μM peptide concentration, values that are superior to that for 9,10-anthraquinone (30% at 100 μM).[35] On the other ~~side~~hand, compound **1a** ~~, displays μM binding~~ displayed micromolar affinity for BuChE~~,~~ and 58% ~~percentage of~~percent inhibition of ~~the~~ fibril formation. Nevertheless, none of the carbazole and aniline containing compounds~~, which~~ that were originally shown to be neuroprotective and neurogenerative in mice~~,~~[8] resulted in multitarget leads across all of the chosen amyloid cascade targets.

**Table 2.** Experimental ~~results for~~Results of the ~~multitarget assays.~~Multitarget Assays

| ~~Compound~~ compound | *Ee*AChE | | hsBuChE | | $^{K}$Aβ(1−40)$^{T}$ ~~Aβ(1-40)~~ | BACE-1 | |
|---|---|---|---|---|---|---|---|
| | % Inh. @ ~~10μM$^{K}$10 μM$^{T}$~~ | $IC_{50}$ ~~($^{K}$(μM)$^{T}$ μM)~~ | % Inh. @ ~~10μM$^{K}$10 μM$^{T}$~~ | $IC_{50}$ ~~($^{K}$(μM)$^{T}$ μM)~~ | % Inh. @ ~~100μM$^{K}$100 μM$^{T}$~~ | % Inh. @~~100μM~~ $^{K}$100 μM$^{T}$ | $IC_{50}$ ~~($^{K}$(μM)$^{T}$ μM)~~ |
| **1a** | ~~30$^{K}$30 ± 1$^{T}$ ± 1~~ | ~~–~~–~~–~~ | ~~–~~–~~–~~ | ~~6.0$^{K}$6.0 ± 1.0$^{T}$ ± 1.0~~ | ~~58$^{K}$58 ± 2$^{T}$ ± 2~~ | ~~1.3$^{K}$1.3 ± 0.3$^{T}$ ± 0.3~~ | ~~–~~–~~–~~ |
| **1b** | ~~22$^{K}$22 ± 1$^{T}$ ± 1~~ | ~~–~~–~~–~~ | ~~34$^{K}$34 ± 1$^{T}$ ± 1~~ | ~~–~~–~~–~~ | ~~51$^{K}$51 ± 5$^{T}$ ± 5~~ | ~~2.4$^{K}$2.4 ± 1.4$^{T}$ ± 1.4~~ | ~~–~~–~~–~~ |
| **1c** | ~~49$^{K}$49 ± 2$^{T}$ ± 2~~ | ~~–~~–~~–~~ | ~~33$^{K}$33 ± 1$^{T}$ ± 1~~ | ~~–~~–~~–~~ | ~~36$^{K}$36 ± 5$^{T}$ ± 5~~ | ~~1.5$^{K}$1.5 ± 0.3$^{T}$ ± 0.3~~ | ~~–~~–~~–~~ |
| **1d** | ~~15$^{K}$15 ± 1$^{T}$ ± 1~~ | ~~–~~–~~–~~ | ~~12$^{K}$12 ± 1$^{T}$ ± 1~~ | ~~–~~–~~–~~ | ~~41$^{K}$41 ± 3$^{T}$ ± 3~~ | ~~1.6$^{K}$1.6 ± 1.5$^{T}$ ± 1.5~~ | ~~–~~–~~–~~ |
| **1e** | ~~–~~–~~–~~ | ~~7.2$^{K}$7.2 ± 0.4$^{T}$ ± 0.4~~ | ~~20$^{K}$20 ± 1$^{T}$ ± 1~~ | ~~–~~–~~–~~ | ~~46$^{K}$46 ± 3$^{T}$ ± 3~~ | ~~0.5$^{K}$0.5 ± 0.3$^{T}$ ± 0.3~~ | ~~–~~–~~–~~ |

| ~~Compound~~ compound | *Ee*AChE | | hsBuChE | | ~~Aβ(1-40)~~ Aβ(1−40) | BACE-1 | |
|---|---|---|---|---|---|---|---|
| | % Inh. @ ~~10μM~~ 10 μM | $IC_{50}$ ~~(~~(μM)~~)~~ | % Inh. @ ~~10μM~~ 10 μM | $IC_{50}$ ~~(~~(μM)~~)~~ | % Inh. @ ~~100μM~~ 100 μM | % Inh. @~~100μM~~ 100 μM | $IC_{50}$ ~~(~~(μM)~~)~~ |
| **1f** | ~~–~~ | ~~7.8~~7.8 ± 0.2 ~~± 0.2~~ | ~~10~~10 ± 1 ~~± 1~~ | ~~–~~ | ~~49~~49 ± 1 ~~± 1~~ | ~~0.9~~0.9 ± 0.9 ~~± 0.9~~ | ~~–~~ |
| **3e** | ~~48~~48 ± 1 ~~± 1~~ | ~~–~~ | ~~–~~ | ~~1.1~~1.1 ± 0.2 ~~± 0.2~~ | ~~11~~11 ± 3 ~~± 3~~ | ~~–~~ | ~~3.1~~3.1 ± 0.4 ~~± 0.4~~ |
| **3f** | ~~–~~ | ~~14~~14 ± 1 ~~± 1~~ | ~~–~~ | ~~7.1~~7.1 ± 0.7 ~~± 0.7~~ | ~~28~~28 ± 3 ~~± 3~~ | ~~–~~ | ~~3.1~~3.1 ± 0.3 ~~± 0.3~~ |

Finally, ~~as seen from~~ this table shows that the benzylamine ~~amine~~ -bearing compounds (**3e** and **3f**) have improved ~~their affinity~~affinities for BACE-1 by ~~three~~3 orders of magnitude over the aniline -containing compounds. This result validates and supports the outcome of our calculations (see Figures 5 and 6), which indicate that the addition of a $CH_2$ fragment provides hits across the set of scoring functions used in our calculations. As mentioned before, this effect is probably due to the ~~raise in the~~larger p$K_a$ ~~in~~of the benzylamine's amino group, which favors the formation of an ion pair with one of the Asp residues of the active -site Asp dyad. These latter compounds (**3e** and **3f**) have improved ~~their~~ affinity for BuChE, and **3f** also displays ~~as well a~~ micromolar affinity for AChE. Nevertheless, their ~~Abeta~~Aβ aggregation inhibition ~~has~~ dropped below the 30% inhibition displayed by the reference compound (9,10-anthraquinone).

**2.** Screening ~~a third generation candidates~~of Third-Generation Candidates: Indole ~~based multitarget candidates~~-Based Multitarget Candidates

The carbazole moiety present in the candidates synthesized and assayed above is quite a bulky group. Perusal of the resulting binding poses showed some steric clashes between the ligand and some protein side chains. The close van der Waals contacts are allowed by the GOLD docking protocol as a way of compensating for the lack of protein flexibility.[15] Figures S1 and S2 display the steric clashes of some ligands with BACE-1 and AChE. An option to avoid the steric clashes altogether ~~will~~would be to search for a smaller aromatic ~~groups~~group in place of the carbazole, ~~like~~such as an indole. ~~Based on~~On the basis of this idea, we designed a new generation of multitarget candidates bearing this fragment ~~in~~at one end and ~~in~~ the ~~other end the~~ same aromatic moieties ~~which were already~~ used in the previous sections (substituted anilines and benzylamines) at the other end. For these ligands we ~~have chosen~~chose the OBn substituent for the anilines and benzylamines~~, since~~ because the analysis of the results for the carbazole-containing compounds described above ~~has shown~~showed that this substituent provides ~~the~~ leads with the right length to span the distance from the CAS to the PAS in AChE.

**2.1.** BACE-1 ~~ligand screening~~Ligand Screening. Figure 12 lists the global hit success for the indole-based derivatives, while the scoring function values for this set of compounds are listed in Tables S6 and S7. The structural variables analyzed in these figures are the same as in the study of the carbazole derivatives in the previous section and include the moiety to which the amino group belongs (aniline or benzylamine), its protonation state, the substitution of the indole group, the substituent position (ortho or meta) ~~of~~on the other aromatic ring, and the stereochemistry of the OH group.

Perusal of our results indicates that the indole-based ligands have a higher probability of binding to BACE-1 with a medium -open or fully open flap (see Tables S6 and S7). The ~~number~~numbers of hits with a closed flap ~~is~~are very small, especially when using ~~a~~the ChemPLP scoring function, indicating that these molecules fit in the active site of BACE-1 thanks to the plasticity of its flap.

In the case of the carbazole-based compounds, the best -ranking ~~compounds where~~ones were those that contained a benzylamine moiety, one that assured the existence of a protonated amino group. A global comparison of the indole-based compounds ~~that contain~~containing an aniline (~~see~~ Figure 12, ~~upper~~top panel) with those ~~that contain~~containing a benzylamine (Figure 12, ~~lower~~bottom panel) indicate that the latter present a larger global hit rate, a pattern similar to that observed for the carbazole -containing compounds. Nevertheless, the preferred benzylamine substitution pattern in the indole-based compounds ~~(~~predicted by our calculations~~)~~ differs from the one predicted for the carbazole -containing ligands, since these latter compounds favor an ortho rather than meta substitution pattern for benzylamines. On the other hand, perusal of Figure 12 suggests that the indole-based compounds ~~favors a~~favor meta

over the ortho substitution, a substitution pattern also followed by the aniline -bearing compounds. Moreover, for these latter compounds, the largest increase is observed for the hits containing a neutral ligand.

**Figure 12.** Global hit success that resultresulting from the docking to BACE-1 of indole derivatives, anilines bearing (upper panel top) anilines and benzylamines (lower panel bottom) benzylamines.

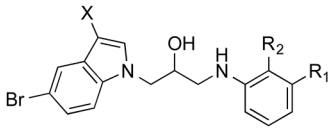


**4a**: $R_1$ = H, $R_2$ = OBn, X = H
**4b**: $R_1$ = H, $R_2$ = OBn, X =Br
**4c**: $R_1$ = H, $R_2$ = OBn, X = Me
**5a**: $R_1$ = OBn, $R_2$ = H, X = H
**5b**: $R_1$ = OBn, $R_2$ = H, X =Br
**5c**: $R_1$ = OBn, $R_2$ = H, X = Me

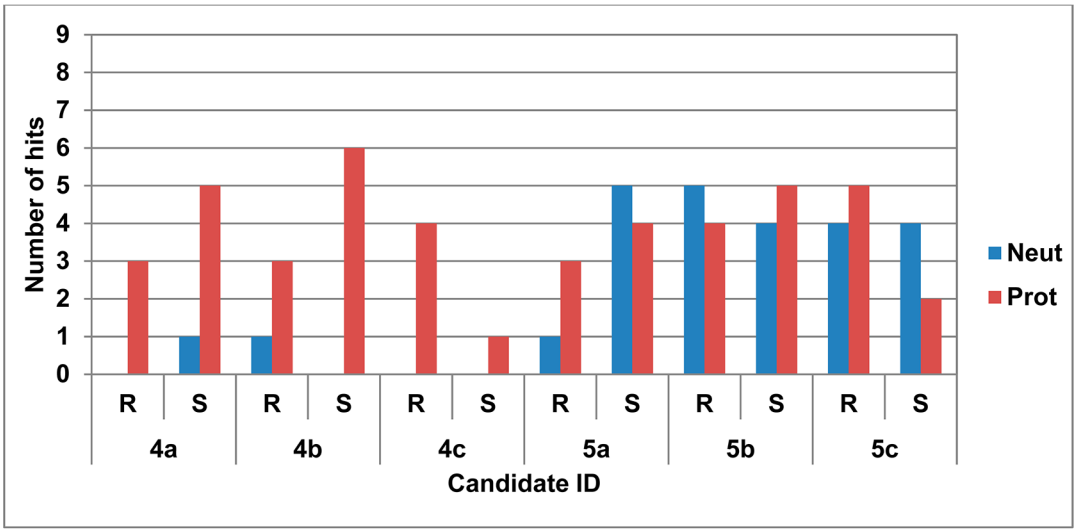


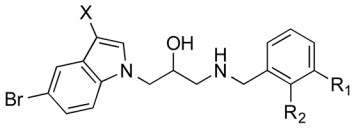


**6a**: $R_1$ = H, $R_2$ = OBn, X = H
**6b**: $R_1$ = H, $R_2$ = OBn, X =Br
**6c**: $R_1$ = H, $R_2$ = OBn, X = Me
**7a**: $R_1$ = OBn, $R_2$ = H, X = H
**7b**: $R_1$ = OBn, $R_2$ = H, X =Br
**7c**: $R_1$ = OBn, $R_2$ = H, X = Me

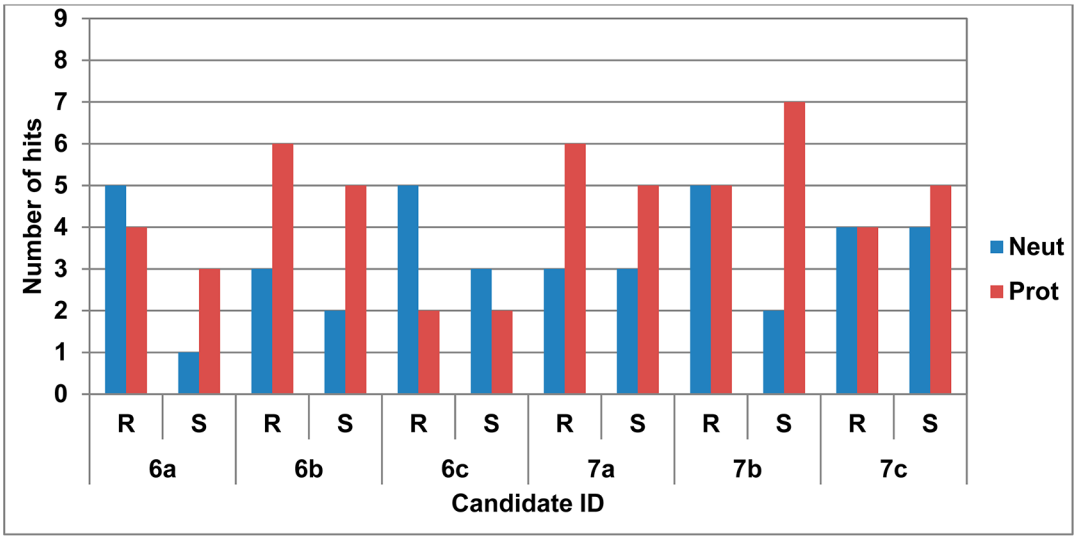

We have also studied the effect of the ligand protonation state on the number of hits. For both the aniline as well as the- and benzylamine -containing compounds (Figure 12), the number of hits increasesis larger (for the most part) when the amino group is protonated, rather than neutral.

**2.2.** AChE ligand screeningLigand Screening. The global hit rate resulting from the AChE -docking -based screening calculations for the indole derivatives that contain a substitutedcontaining an aniline or benzylamine insubstituted at the ortho or meta positionsposition are depicted in Figure 1313 . Comparison of the effecteffects of the substitution pattern infor both aniline and benzylamine (shown in this figure) indicateindicates that changing the substitution from ortho to meta increases the number of hits. As can be seen from Figure 1313 , the number of hits obtained and the consensus reached across the three scoring functions indicate that our indolebenzylamineindole- and benzylamine-containing compounds fit well inside AChE, spanning both the main site (CAS) and the peripheral one (PAS). Moreover, comparison of the aniline -bearing compounds with the benzylamine-bearing ones indicateindicates that the latter present a larger number of hits across all three scoring functions, probably due to anbecause of the increase in the size of the ligands that allowallows them to span better boththe two binding sites better.

**Figure 13.** (a) AChE docking results for indole-bearing compounds with (top) ortho- and (bottom) meta-substituted anilines. (b) AChE docking results for indole-bearing compounds with (top) ortho- and (bottom) meta-substituted benzylamines.

a)

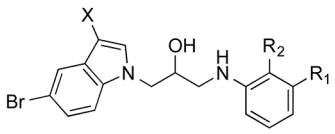


**4a**: $R_1$ = H, $R_2$ = OBn, X = H
**4b**: $R_1$ = H, $R_2$ = OBn, X =Br
**4c**: $R_1$ = H, $R_2$ = OBn, X = Me
**5a**: $R_1$ = OBn, $R_2$ = H, X = H
**5b**: $R_1$ = OBn, $R_2$ = H, X =Br
**5c**: $R_1$ = OBn, $R_2$ = H, X = Me

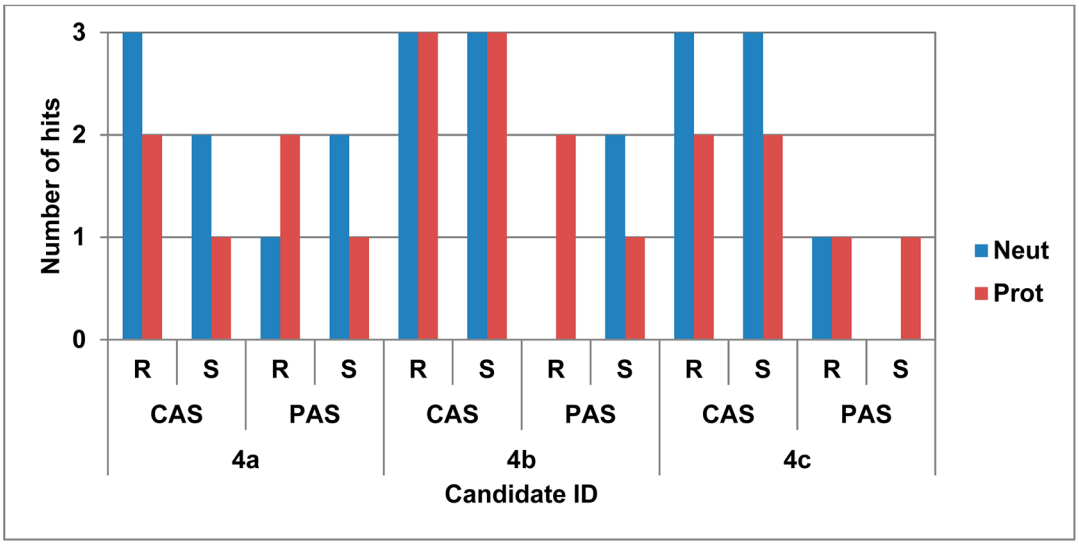


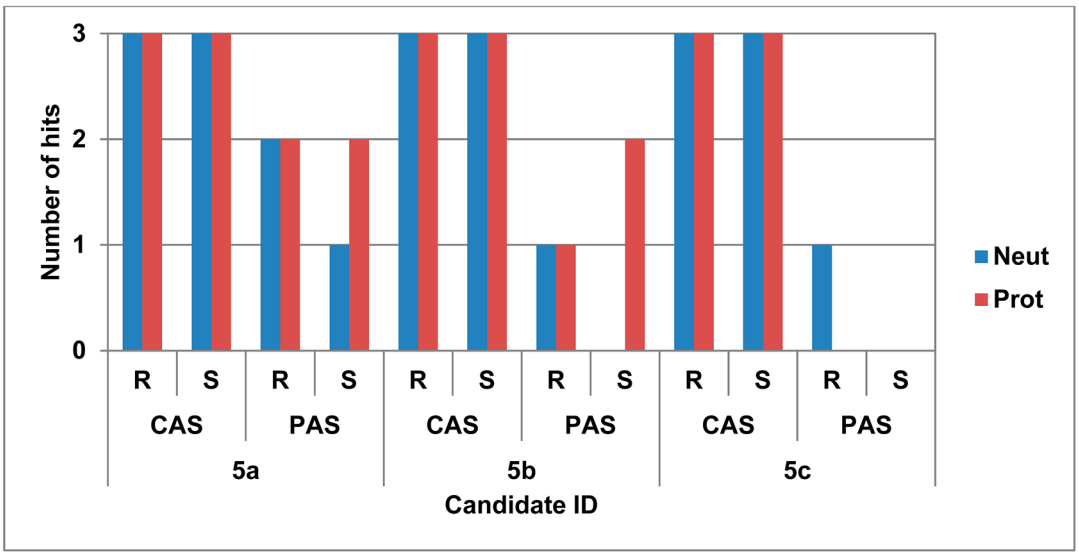

b)

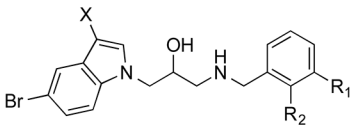


**6a**: $R_1$ = H, $R_2$ = OBn, X = H
**6b**: $R_1$ = H, $R_2$ = OBn, X =Br
**6c**: $R_1$ = H, $R_2$ = OBn, X = Me
**7a**: $R_1$ = OBn, $R_2$ = H, X = H
**7b**: $R_1$ = OBn, $R_2$ = H, X =Br
**7c**: $R_1$ = OBn, $R_2$ = H, X = Me

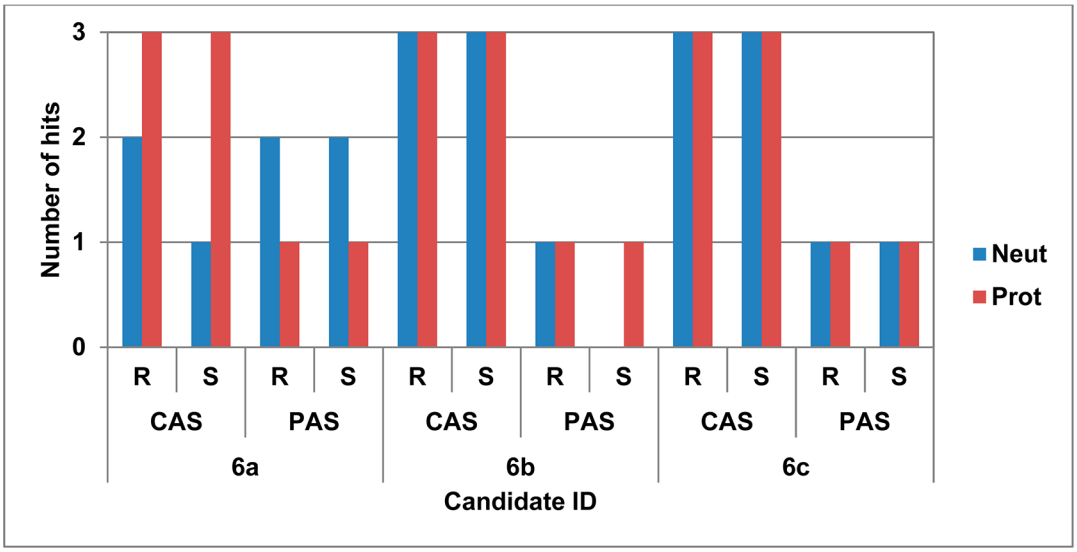


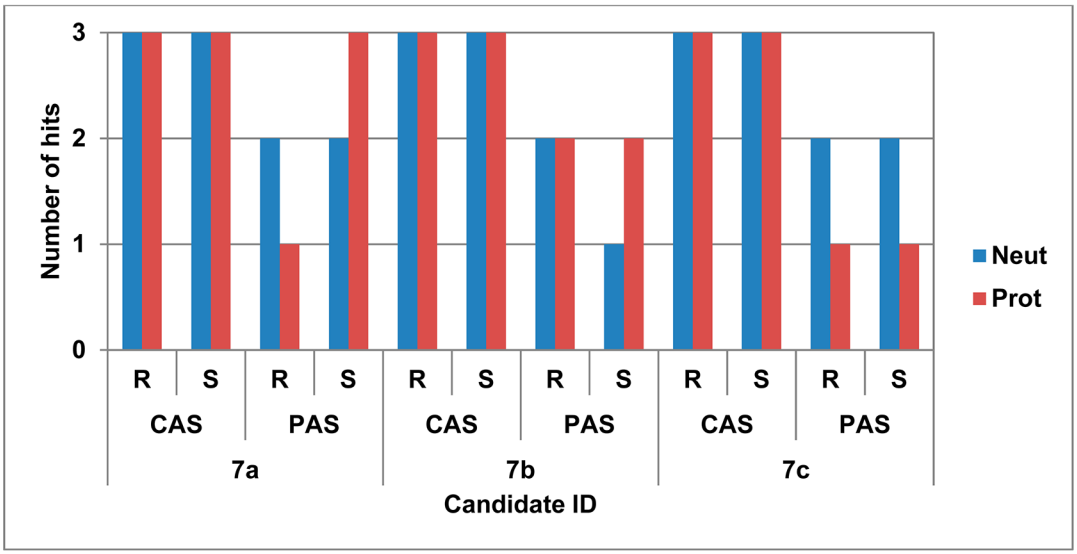


One interesting issue is the docking exit poses. As we mentioned above in our pharmacophore depiction for AChE, we seek to have dual inhibitors in which one of the end aromatic fragments is to be found at the CAS and the other end aromatic group positions itself in the PAS, both producing π -stacking interactions with the aromatic residue clusters residing in ~~both~~these two sites (see Figure 1). There are two possible pose orientations that fulfill this hit. In the first one, the indole moiety is predicted to be found in the CAS while the terminal benzyloxy group is to be found at the PAS. In the second possible pose, we have the inverse option in which the indole fragment resides at the PAS. ~~We have listed~~In Figure 13 ~~in Figure 13~~we have listed both poses and ~~have~~ referred to them as ~~"~~"CAS~~"~~" and ~~"~~"PAS~~"~~",

respectively. As seen fromshown in these plots, the numbernumbers of ‘“CAS”’ hits (indole docked into the CAS) isare larger than those when the one that places this fragmentindole fragment is placed in the PAS (for both forthe aniline- and benzylamine -containing compounds), a result that we will try to verify through X-ray crystallography. In Figure 14 we depict the most favored pose obtained for compound **7a** with the ChemscoreChemScore fitness function. NoticeIt should be noted that the indole fits neatly ininto the CAS, making π -stacking interactions with residues W84 and F330, while the Bn group interacts with W279 and Y70 in the PAS.

Finally, our results (shown in Figure 13) indicate that there is scarcely a preference for one of the enantiomers, neither there is a clear proclivity for a neutral or charged state for the amino group.

**Figure 13a.** Docking results of the indole bearing compounds with *ortho* (upper panel) and *meta* (lower panel) substituted anilines on AChE.

**Figure 13b.** Docking results for indole bearing compounds with *ortho* (upper panel) and *meta* (lower panel) substituted benzylamines on AChE.

**Figure 14.** Pose for ligand **7a** in which the indole fragment interacts (through π stacking) with residues Trp 84 and Phe 330 in the CAS, while the treminal Bn group interacts with Tyr 70 and Trp 279 at the PAS site.

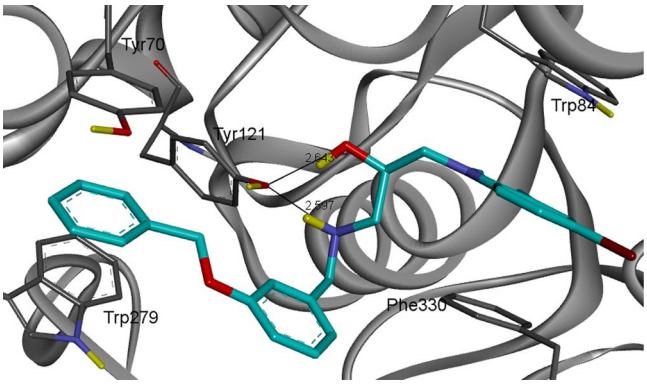


Finally, the results shown in Figure 13 indicate that there is scarcely a preference for one of the enantiomers and that there is no clear proclivity for a neutral or charged state for the amino group.

**2.3.** Inhibitor Aβ12–28 peptide interaction resultsPeptide Interaction Results. We have performed the MD simulations on three of our indole candidates: one containing an aniline fragment (**4b**) and the other two containing a benzylamine moiety (**7b** and **7c**). The results indicate that percentage residency times around the peptide with 7.5 Å radii for these compounds are relatively high (88 ± 2.0, 96 ± 2.0 and 86 ± 1.3 respectively).

We performed MD simulations on three of our indole candidates: one containing an aniline fragment (**4b** ) and the other two containing a benzylamine moiety (**7b** and **7c** ). The results indicate that the percentage residence times around the peptide with 7.5 Å radii for these compounds are relatively high (88 ± 2.0, 96 ± 2.0, and 86 ± 1.3%, respectively). Figure 15 displays the ligands residency timeligand residence times around every residue of Aβ12–28. As seen fromshown in this figure, the ligands favor two binding spots (populated by aromatic residues), a result already observed for the carbazole -containing compounds. The most frequented site is around the LVFFA segment, and the second one contains the two His residues at the start of the sequence. Another important feature is that these ligands present much higher residence times than the reference ligand, the 9,10-anthraquinone, a compound that has a 30% fibril formation inhibition at 100 μM concentration. Furthermore, comparison of the intra-peptideintrapeptide residue interactioninteractions when these two ligands are present (see Figures 16 and S4) with the residue contactcontacts when they are absent (see Figures 11 and S4) indicates that these compounds clearly interrupt the formation of the hairpin structures that are the hallmark of Aβ peptide aggregates, indicating that these ligands may inhibit amyloid aggregation. Finally, we predict that the benzylamine-containing compounds (**7b** and **7c**) reduce the formation of turns (around the DVSG segment) more efficiently than the aniline -based compound (**4b**).

**Figure 15.** Ligand–peptide residues fractionresidue contact timestime fractions. Cut-offThe cutoff distance iswas set at 4.5 ÅÅ.

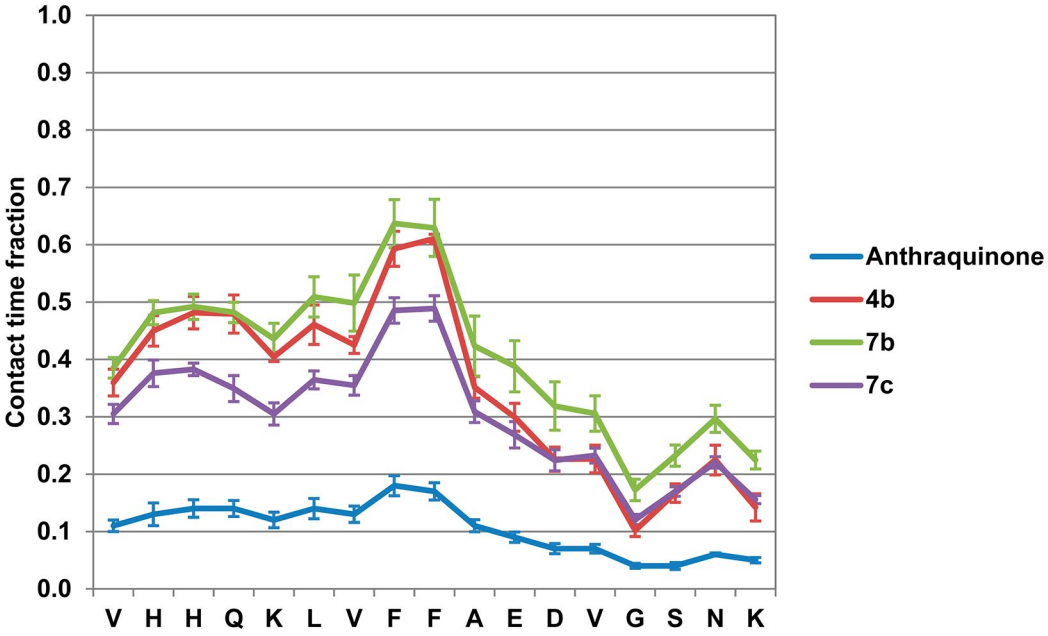


**Figure 16.** Residue–residue interaction contact ~~map~~maps in the presence of candidates **4b**, **7b** , and **7c**. ~~Cut-off~~The cutoff interaction distance ~~is~~was set at 4.5 ~~Å~~Å. The color scale shown ~~above~~at the bottom indicates the residence times.

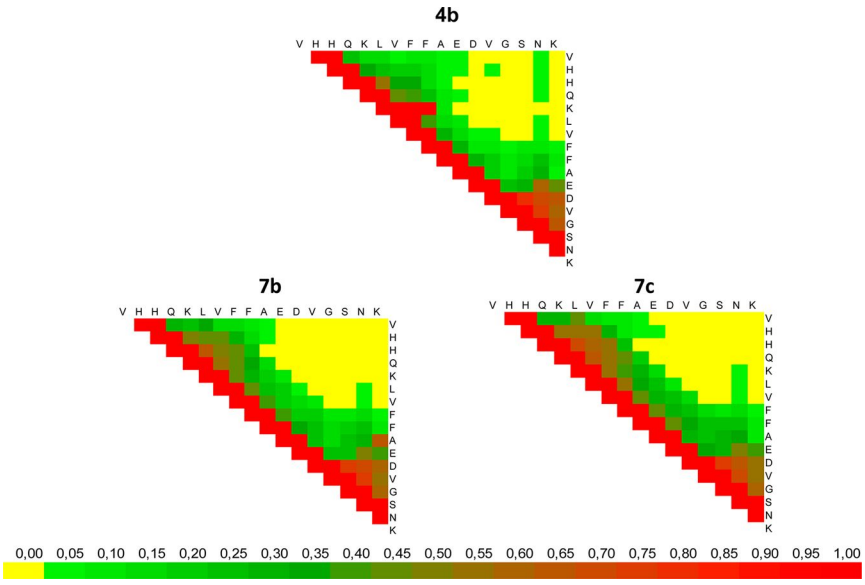


**2.4.** Synthesis and ~~experimental assays~~Experimental Assays for ~~indole containing compounds~~Indole-Containing Compounds. The indole derivatives whose structures contain ~~either~~ an aniline or ~~a~~ benzylamine fragment were obtained by the same synthetic route as the carbazole -containing compounds, as indicated in Scheme 2, which includes the list of synthesized molecules.

**Scheme 2.** Synthetic ~~route~~Routes and ~~indole derivatives synthesized.~~ Indole Derivatives Synthesized

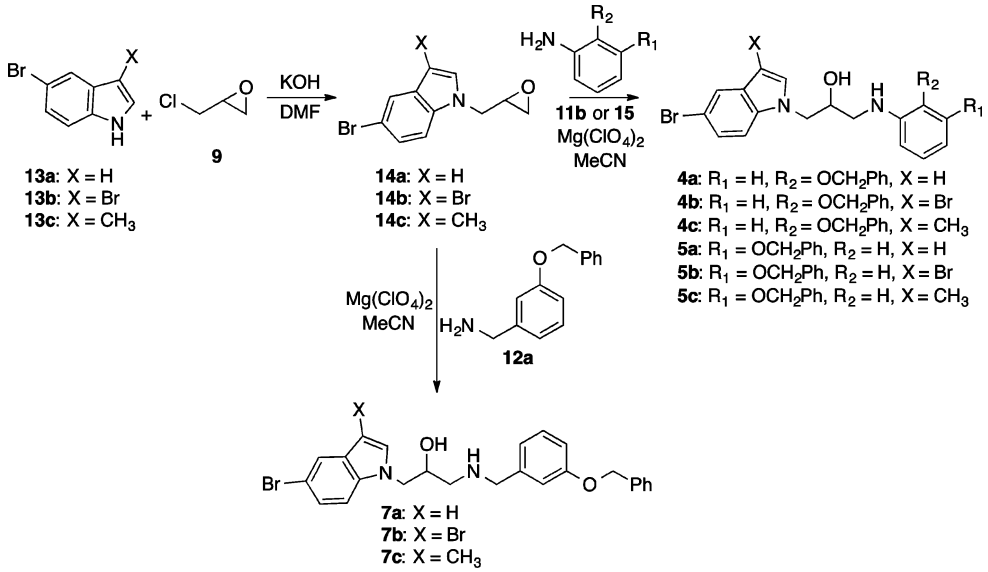


The results of the binding assays to BACE-1, AChE, and BuChE for the selected compounds~~, together with~~ as well as the fibril inhibition ~~assay~~assays are listed in Table 3. As ~~seen from~~shown in this table, the meta -substituted benzylamine compounds display altogether higher ~~activity~~activities than the ortho -substituted aniline ones for AChE, a result that validates the predictive power of our in silico protocol presented above. More importantly, the replacement of ~~a~~the carbazole moiety by an indole moiety with a ~~benzylamine~~ meta-substituted ~~in~~benzylamine ~~metaled has lead~~ to candidates that bind to *all* of the chosen amyloid cascade targets~~,~~ (BACE-1, amyloid aggregates, and the peripheral site in AChE~~),~~ as well as to AChE's main site and BuChE, implying also a positive cholinergic effect in AD. Hence, compounds ~~like~~such as **7c** are truly multitarget compounds.

~~Finally, the results displayed in Tables 2 and 3 also afford us with important structural information for the binding poses of both carbazole and indole bearing compounds to the cholinergic targets. For instance compounds **7a**, **7b** and **7c** bind even better to BuChE than to AChE. This result has structural implications, since these two enzymes are highly homologous in the CAS, but BuChE replaces the targeted aromatic residues present in the PAS site of AChE by non-aromatic ones, precluding the formation of possible π stacking interactions in this enzyme.[36] Hence, the fact that there are ligands that bind to both cholinesterases may mean that they are able to diffuse to the CAS site in AChE and bind to it. This experimental results support the idea that our design has produced dual AChE inhibitors that bind both to the CAS and the PAS of this enzyme, a conclusion reached as well by the pose search in our docking based screening simulations (see Figures 13 and 14).~~

**Table 3.** Experimental ~~results~~Results for ~~indole based compounds.~~Indole-Based Compounds

| ~~Candidate~~ | *Ee*AChE | | hsBuChE | | Aβ(~~1~~–40) | | BACE-1 | |
|---|---|---|---|---|---|---|---|---|
| candidate | % Inh. @ ~~10μM~~[K]10 μM[T] | IC50 ~~([K](μM)[T] μM)~~ | % Inh. @ ~~10μM~~[K]10 μM[T] | IC50 ~~([K](μM)[T] μM)~~ | % Inh. @ ~~100μM~~[K]100 μM[T] | IC50 ~~([K](μM)[T] μM)~~ | % Inh. @~~100μM~~ [K]100 μM[T] | IC50 ~~([K](μM)[T] μM)~~ |
| **4a** | ~~44[K]44 ± 1[T] ± 1~~ | ~~–[–]~~ | ~~17[K]17 ± 3[T] ± 3~~ | ~~–[–]~~ | ~~43[K]43 ± 1[T] ± 1~~ | ~~–[–]~~ | ~~5.7[K]5.7 ± 1.6[T] ± 1.6~~ | ~~–[–]~~ |
| **4b** | ~~45[K]45 ± 2[T] ± 2~~ | ~~–[–]~~ | ~~18[K]18 ± 3[T] ± 3~~ | ~~–[–]~~ | ~~23[K]23 ± 2[T] ± 2~~ | ~~–[–]~~ | ~~6.3[K]6.3 ± 1.4[T] ± 1.4~~ | ~~–[–]~~ |
| **4c** | ~~44[K]44 ± 1[T] ± 1~~ | ~~–[–]~~ | ~~19[K]19 ± 1[T] ± 1~~ | ~~–[–]~~ | ~~43[K]43 ± 5[T] ± 5~~ | ~~–[–]~~ | ~~16.4[K]16.4 ± 0.1[T] ± 0.1~~ | ~~–[–]~~ |

| Candidate | *Ee*AChE | | hsBuChE | | Aβ(1–40) | | BACE-1 | |
|---|---|---|---|---|---|---|---|---|
| candidate | % Inh. @ 10μM[K] 10 μM[T] | $IC_{50}$ ([K](μM)[T] μM) | % Inh. @ 10μM[K] 10 μM[T] | $IC_{50}$ ([K](μM)[T] μM) | % Inh. @ 100μM[K] 100 μM[T] | $IC_{50}$ ([K](μM)[T] μM) | % Inh. @100μM [K]100 μM[T] | $IC_{50}$ ([K](μM)[T] μM) |
| **5a** | – – | 8.5[K] 8.5 ± 0.7[T] ± 0.7 | 20[K] 20 ± 2[T] ± 2 | – – | 55[K] 55 ± 3[T] ± 3 | – – | 3.5[K] 3.5 ± 2.4[T] ± 2.4 | – – |
| **5b** | – – | 9.3[K] 9.3 ± 0.6[T] ± 0.6 | 24[K] 24 ± 1[T] ± 1 | – – | 22[K] 22 ± 2[T] ± 2 | – – | 1.8[K] 1.8 ± 0.6[T] ± 0.6 | – – |
| **5c** | – – | 12[K] 12 ± 1[T] ± 1 | 17[K] 17 ± 1[T] ± 1 | – – | 57[K] 57 ± 2[T] ± 2 | – – | 0.1[K] 0.1 ± 0.1[T] ± 0.1 | – – |
| **7a** | – – | 10.4[K] 10.4 ± 0.1[T] ± 0.1 | – – | 0.70[K] 0.70 ± 0.02[T] ± 0.02 | 57[K] 57 ± 3[T] ± 3 | – – | – – | 3.0[K] 3.0 ± 1.4[T] ± 1.4 |
| **7b** | – – | 9.1[K] 9.1 ± 1.1[T] ± 1.1 | – – | 0.29[K] 0.29 ± 0.05[T] ± 0.05 | 47[K] 47 ± 2[T] ± 2 | – – | – – | 2.5[K] 2.5 ± 0.1[T] ± 0.1 |
| **7c** | – – | 5.9[K] 5.9 ± 1.0[T] ± 1.0 | – – | 0.39[K] 0.39 ± 0.03[T] ± 0.03 | 78[K] 78 ± 1[T] ± 1 | 34[K] 34 ± 2[T] ± 2 | – – | 4.3[K] 4.3 ± 0[T] ±0 .80.8 |

Finally, the results displayed in Tables 2 and 3 also afford us with important structural information about the binding poses of both carbazole- and indole-bearing compounds with the cholinergic targets. For instance compounds **7a**, **7b**, and **7c** bind even better to BuChE than to AChE. This result has structural implications, since these two enzymes are highly homologous in the CAS but BuChE replaces the targeted aromatic residues present in the PAS of AChE by nonaromatic ones, precluding the formation of possible π-stacking interactions in this enzyme.[36] Hence, the fact that there are ligands that bind to both cholinesterases may mean that they are able to diffuse to the CAS site in AChE and bind to it. These experimental results support the idea that our design has produced dual AChE inhibitors that bind both to the CAS and the PAS of this enzyme, a conclusion reached as well by the pose search in our docking-based screening simulations (see Figures 13 and 14).

## DISCUSSION & CONCLUSIONSDiscussion and Conclusions

As mentioned in the introductionIntroduction , the search for single leads for all of the chosen amyloid cascade targets represents a sizable challenge due tobecause of the substantial differences in their binding sites. To tackle this issue, we have proposed a two-step protocol. In the first step we have designed a pharmacophore, built around the knowledge obtained in our lab and others, that includes the interactions with the molecular targets that the candidates should fulfill. The resulting template allowsallowed for the automated screening of multiple candidates using programs likesuch as ZINCPharmer.[37] Our search for compounds in bibliographical data sets led us to a group of carbazole -containing compounds with substituted aniline fragments, which have been that were previously identified as neuroprotective and neurogenerative compounds in mice.[8]

The second step of our method includesincluded the evaluation and optimization of the initial set of compounds by a computer-assisted protocol that combines docking calculations for the enzyme targets (BACE-1 and AChE) with MD simulations for the in silico study of AbetaAβ aggregation inhibition. The results of the docking calculations rely not only rely on obtaining the best -scoring compounds, but more importantly on fulfilling the pattern of interactions with the cardinal residues in our targets as shown in our pharmacophore scheme (see Figure 1). The MD simulations used for amyloid aggregation inhibition studied the time evolution of an amyloid peptide fragment in the presence and absence of our candidates, aimed atwith the aim of determining the strength of the binding to ""hot spot²" peptide fragments, as well as understanding and evaluating the effect of the candidates on the peptide secondary structure.

Our computer-aided protocol was used with a twofold aim. Firstly,: (1) to investigate ifwhether the original compounds owed their known biologicbiological activity to their binding to some of the amyloid cascade targets, and secondly(2) to search for analogues with an increased affinityaffinities for the largest possible group of amyloid cascade targets. The first round of calculations on our original compounds (that purportedly had neuroprotective and

neurogenerative properties) displayed very few hits in BACE-1 (see Figure 5), but a number of hits in AChE. Our binding assays (Table 2) corroborated the outcome of our calculations, since the initial set of compounds displayed low affinities for BACE-1 (not surpassing the 33% BACE-1 inhibition at 1mM1 mM). Nevertheless, as predicted by our calculations these compounds presented μM, micromolar affinity for AChE forwas exhibited by those compounds that presentpresenting the largest scoring function values in our docking calculations (see the results for **1e** and **1f** in Figure 7). Perusal of the exit docking poses indicates that these compounds are able to span boththe two AChE binding sites, a result that could explain their better affinity as compared towith their congeners. Finally, some of the compounds in the initial set display adisplayed fibril formation inhibition slightly above that of the reference compound 9,10-anthraquinone.[35]

In order to improve the binding across the amyloid targets and especially for BACE-1, we proceeded to modify these compounds with the information afforded by two computer -aided design cycles. The initial screening results for BACE-1 anticipated that most of the hits were obtained with the protonated amino group in the aniline (see Figure 5). In order to increase the probability that the amino group willwould actually be protonated, we replaced the aniline moiety by a benzylamine fragment. The docking results predicted that the second-generation compounds should improve theirhave improved hit rates mainly for BACE-1. In order to test this outcome, we synthesized and assayed two of the benzylamine -containing compounds that showed promising results in the docking calculations (**3e** and **3f**). The binding assays indicated that the new candidates had improved their binding affinities for BACE-1 by more than 3 orders of magnitude ($IC_{50}$ = 3.1 μM). Interestingly enough, these compounds also showed affinity for BuChE. In healthy brains, AChE hydrolyzes about 80% of acetylcholine while BuChE plays a secondary role. However, as AD progresses, the activity of AChE is greatly reduced in specific brain regions while the BuChE activity increases, likely as a compensation for the AChE depletion.[38] Consequently, both enzymes are useful therapeutic targets for AD, and our experimental results indicate that our compounds not only should affect the amyloid cascade at the core of the AD, but also should have a positive cholinergic effect.[38]

The design of the third -generation ligands was afforded bybased on the inspection of the exiting poses of the carbazole -containing compounds, which showed that there waswere some steric clashes between the carbazole moiety and some of the residues belonging either to BACE-1 andor AChE (see Figures S1 and S2). In order to avoid close van der Waals overlaps, we designed a new set of ligands in which the carbazole moiety was replaced by indole, a smaller fragment, while at the other end we kept the substituted aniline or benzylamine fragments. Even in the case of the aniline -containing compounds, the replacement of a carbazole forwith an indole (see Figures 5 and 12) increases substantially increases the number of hits for BACE-1, especially when the ligand is neutral. Moreover, we predict that an additional hit enrichment could be obtained by replacing the aniline moiety by a benzylamine fragment substituted at the meta position rather than at the ortho position (see Table S7 and Figure 12). Our docking calculations show that AChE has a very similar inhibitor preference as BACE-1, meaning that a consensus inhibitor design for the two enzymes has been reached for both enzymes.

ThereA sizable effort has been a sizable effort indevoted to understanding the effect of ligands on the secondary structure of AbetaAβ peptides by MD simulations, in order to getgain some insight ontointo the inhibitory effect of these ligands.[28] For instance, Wang et al.[39] studied the time evolution of the Aβ peptide in the presence of polyphenolic xanthonesxanthones. The analysis of rather short MD simulations (in the nanosecond regime) indicated that the presence of these ligands seem to help retain the alpha α-helix secondary structure (from which these simulations startstarted) and hence preclude amyloid aggregation. On the other hand, the results of our calculations shed light on an open question that relates to the existence of an amyloidogenic core whichthat serves as a template for amyloid oligomers and fibril formation, an issue that is relevant not only to AD but also to other pathologies (e.g., diabetes type -2 diabetes and Parkinson's disease) that are associated with the misfolding of polypeptides.[40] Hence, a possible paradigm for an AbetaAβ aggregation route inhibition route could rely on precluding the emergence of the template structure with a beta β-hairpin structure (around the DVGS motif) observed in various NMR experiments.[41] Comparison of the results obtained from our MD simulations of an Aβ fragment (residues 12 to 28) in the presence and absence of our candidate compounds seemseemed to indicate that the best aggregation inhibitors are able to modulate the secondary structure of the peptide, partially precluding the formation of a hairpin aggregation core. Perusal of Figures 10 and 15 indicateindicates that the modulation of the secondary structure of the AbetaAβ peptide is achieved by interaction of the ligand with the pairs of aromatic residues (predominantly Phe19–Phe20) present in the peptide segment studied. It was found that the hydrophobic interactions that involve these aromatic residues are vital for the genesis of the hairpin structure through the collapse of the hydrophobic stretch Leu17–Ala21.[41] The only other aromatic residues present

in the full ~~Abeta~~Aβ peptide are single ~~aminoacids~~amino acids that are located in the segment ~~comprised by~~comprising the first ~~eleven~~11 residues~~, that~~ (which is known to lack any structure in peptide aggregates~~,~~) and hence possibly do not have any role in inducing aggregation. Figure S3 displays a snapshot of the interaction between compound **7b** and the Aβ12~~–~~–28 peptide~~,~~ as obtained from the MD simulation. As ~~seen from~~shown in this figure, there is a π -stacking interaction between the aromatic core of the benzylamine fragment and one of the aromatic residues mentioned above.

We ~~have~~ calculated the variability, as given by the standard deviation (SD), of the crucial contacts between the segments DVGS and VHHQ in the MD trajectory (see Table S8 for some typical examples). The results ~~indicate~~show an increase in the SD values in the absence of a ligand, ~~an outcome that~~which indicates that the presence of our ligands seems to reduce the contact fluctuations, stabilizing secondary structures other than a turn.

There seems to be some relationship between the disruption of the aforementioned turn in our simulations and the result of the ThT assays. For instance, 9,10-anthraquinone, a compound that results in only ~~inhibits~~ 30% inhibition of fibril formation, precludes turn formation to a much lesser extent ~~the turn formation as compared to~~than some of our best compounds ~~like~~, such as **7c**. Moreover, the indole/aniline derivative **4b** is much less effective in precluding the turn template ~~as their~~than the benzylamine analogue **7b**, providing support for our MD simulation results. Nevertheless, we expect that this simple protocol based on MD simulations of a single ~~Abeta~~Aβ peptide fragment may not be able to give a quantitative inhibition ranking~~,~~ but rather would enable us to ~~tell apart~~distinguish the binders from the inactive compounds. Presently~~, we~~ are performing our MD simulations on a larger set of peptide~~–~~–ligand complexes in order to validate the predictive capabilities of our protocol that could be useful in the design of ~~Abeta~~Aβ aggregation inhibitors.

The results of the enzyme FRET assays for BACE-1, AChE, and BuChE~~,~~ as well as ThT fibril formation assays on indole -based compounds with ~~an~~ aniline and meta -substituted benzylamine ~~derivatives~~moieties fully support the outcome of our calculations, indicating that the latter set of compounds (**7a**, **7b** , and **7c**) are by far the most superior candidates ~~with~~, exhibiting highly improved ligand efficiency~~,~~ and ~~display a~~displaying multitarget behavior across the amyloid cascade and cholinergic pathways.

Besides affording robust predictions about the relative affinity of our candidate compounds, our computer -assisted protocol has provided us with valuable structural predictions such as the flap opening in BACE-1 when bound to our inhibitors~~. or~~ and the orientation of the ligands in AChE, issues we are trying to verify by X-ray crystallography.

## Supporting Information

Additional data for docking to BACE-1 and AChE as well as aggregation simulations as described in the text and general materials and methods for syntheses and in vitro biological evaluations. This material is available free of charge via the Internet at http://pubs.acs.org.

The authors declare no competing financial interest.

## Acknowledgments

Financial support from the Ministerio de Economia y Competitividad of Spain (Project CTQ2011-22436) and the Xunta de Galicia (2007/085 and 10CSA209063PR) is gratefully acknowledged. We ~~would like to~~ thank the Center for Supercomputing in Galicia (CESGA) for computer time and ~~to~~ Prof. Amedeo Caflisch for hosting one of us (J.L.D.) for a short -term visit that allowed him to become familiar with the computer simulation protocols used in the study of amyloid aggregation.

~~Supporting Information Available~~

~~Additional data of docking to BACE-1 and AChE, as well as A aggregation simulations, as described in the text. General materials and methods for syntheses and *in vitro* biological evaluation. This material is available free of charge via the Internet at http://pubs.acs.org.~~

## References

(1) Mangialasche, F.; Solomon, A.; Winblad, B.; Mecocci, P.; Kivipelto, M. Alzheimer's disease: ~~clinical~~Clinical trials and drug development. *Lancet Neurol.* **2010**, *9*, 702–716.

(2) Walsh, D. M.; Selkoe, D. J. Deciphering the molecular basis of memory failure in Alzheimer's disease. *Neuron* **2004**, *44*, 181–193.

(3) Selkoe, D. J. Preventing Alzheimer's disease. *Science* **2012**, *337*, 1488–1492.

(4) Inestrosa, N. C.; Alvarez, A.; Pérez, C. A.; Moreno, R. D.; Vicente, M.; Linker, C.; Casanueva, O. I.; Soto, C.; Garrido, J. Acetylcholinesterase accelerates assembly of amyloid-β-peptides into Alzheimer's fibrils: ~~possible~~Possible role of the peripheral site of the enzyme. *Neuron* **1996**, *16*, 881–891.

(5) (a) Cavalli, A.; Bolognesi, M. L.; Capsoni, S.; Andrisano, V.; Bartolini, M.; Margotti, E.; Cattaneo, A.; Recanatini, M.; Melchiorre, C. A ~~Small~~small molecule targeting the multifactorial nature of Alzheimer's disease. *Angew. Chem., Int. Ed.* **2007**, *46*, 3689–3692. (b) Zhu, Y.; Xiao, K.; Ma, L.; Xiong, B.; Fu, Y.; Yu, H.; Wang, W.; Wang, X.; Hu, D.; Peng, H.; Li, J.; Gong, Q.; Chai, Q.; Tang, X.; Zhang, H.; Li, J.; Shen, J. Design, synthesis

and biological evaluation of novel dual inhibitors of acetylcholinesterase and β-secretase. *Bioorg. Med. Chem.* **2009**, *17*, 1600–1613. (c) Fernández-Bachiller, M. I.; Pérez, C.; Monjas, L.; Rademann, J.; Rodríguez-Franco, M. I. New tacrine-4-oxo-4*H*-chromene hybrids as multifunctional agents for the treatment of Alzheimer's disease, with cholinergic, antioxidant, and β-amyloid-reducing properties. *J. Med. Chem.* **2012**, *55*, 1303–1317.
(6) Viayna, E.; Gómez, T.; Galdeano, C.; Ramírez, L.; Ratia, M.; Badia, A.; Clos, M. V.; Verdaguer, E.; Junyent, F.; Camins, A.; Pallàs, M.; Bartolini, M.; Mancini, F.; Andrisano, V.; Arce, M. P.; Rodríguez-Franco, M. I.; Bidon-Chanal, A.; Luque, F. J.; Camps, P.; Muñoz-Torrero, D. Novel huprine derivatives with inhibitory activity toward β-amyloid aggregation and formation as disease-modifying anti-Alzheimer drug candidates. ~~*Chem. Med. Chem.*~~*ChemMedChem* **2010**, *5*, 1855–1870.
(7) (a) Bolognesi, M. L.; Cavalli, A.; Valgimigli, L.; Bartolini, M.; Rosini, M.; Andrisano, V.; Recanatini, M.; Melchiorre, C. Multi-target-directed drug design strategy: From a dual binding site acetylcholinesterase inhibitor to a trifunctional compound against Alzheimer's disease. *J. Med. Chem.* **2007**, *50*, 6446–6449. (b) Bolognesi, M. L.; Bartolini, M.; Tarozzi, A.; Morroni, F.; Lizzi, F.; Milelli, A.; Minarini, A.; Rosini, M.; Hrelia, P.; Andrisano, V.; Melchiorre, C. Multitargeted drugs discovery: Balancing anti-amyloid and anticholinesterase capacity in a single chemical entity. *Bioorg. Med. Chem. Lett.* **2011**, *21*, 2655–2658. (c) Li, R.-S.; Wang, X.-B.; Hu, X.-J.; Kong, L.-Y. Design, synthesis and evaluation of flavonoid derivatives as potential multifunctional acetylcholinesterase inhibitors against Alzheimer's disease. *Bioorg. Med. Chem. Lett.* **2013**, *23*, 2636–2641.
(8) McMillan, K. S.; Naidoo, J.; Liang, J.; Melito, L.; Williams, N. S.; Morlock, L.; Huntington, P. J.; Estill, S. J.; Longgood, J.; Becker, G. L.; McKnight, S. L.; Pieper, A. A.; De Brabander, J. K.; Ready, J. M. Development of proneurogenic, neuroprotective small molecules. *J. Am. Chem. Soc.* **2011**, *133*, 1428–1437.
(9) Yuan, J.; Venkatraman, S.; Zheng, Y.; McKeever, B. M.; Dillard, L. W.; Sing, S. B. Structure-based design of β-site APP cleaving enzyme 1 (BACE1) inhibitors for the treatment of Alzheimer's disease. *J. Med. Chem.* **2013**, *56*, 4156–4180.
(10) Domínguez, J. L.; Christopeit, T.; Villaverde, M. C.; Gossas, T.; Otero, J. M.; Nyström, S.; Baraznenok, V.; Lindström, E.; Danielson, U. H.; Sussman, F. Effect of the protonation state of the titratable residues on the inhibitor affinity to BACE-1. *Biochemistry* **2010**, *49*, 7255–7263.
(11) Sussman, F.; Villaverde, M. C.; Domínguez, J. L.; Danielson, U. H. On the active site protonation state in aspartic proteases: ~~implications~~Implications for drug design. *Curr. Pharm. ~~Design~~Des.* **2013**, *19*, 4257–4275.
(12) Dvir, H.; Silman, I.; Harel, M.; Rosenberry, T. L.; Sussman, J. L. Acetylcholinesterase: ~~from~~From 3D structure to function. *Chem.-Biol. Interact.* **2010**, *187*, 10–22.
(13) Hopkins, C. R. ACS chemical neuroscience molecule spotlight on dimebon. *ACS Chem. Neurosci.* **2010**, *1*, 587–588.
(14) Yang, W.; Wong, Y.; Ng, O. T. W.; Bai, L.-P.; Kwong, D. W. J.; Ke, Y.; Jiang, Z.-H.; Li, H.-W.; Yung, K. K. L.; Wong, M. S. Inhibition of ~~beta~~β-amyloid peptide aggregation by multifunctional carbazole-based fluorophores. *Angew. Chem.* **2012**, *124*, 1840–1846.
(15) ~~GOLD~~*GOLD* , version 5.1~~,~~; Cambridge Crystallographic Data Centre~~,~~; Cambridge, ~~UK~~U.K..
(16) Jones, G.; Willett, P.; Glen, ~~R.C~~R. C. Molecular recognition of receptor sites using a genetic algorithm with a description of desolvation. *J. Mol. Biol.* **1995**, *245*, 43–53.
(17) Jones, G.; Willett, P.; Glen, R. C.; Leach, A. R.; Taylor, R. Development and validation of a genetic algorithm for flexible docking. *J. Mol. Biol.* **1997**, *267*, 727–748.
(18) Baxter, C. A.; Murray, C. W.; Clark, D. E.; Westhead, D. R.; Eldridge, M. D. Flexible docking using tabu search and an empirical estimate of binding affinity. *Proteins* **1998**, *33*, 367–382.
(19) Eldridge, M. D.; Murray, C. W.; Auton, T. R.; Paolini, G. V.; Mee, R. P. Empirical scoring functions: I. The development of a fast empirical scoring function to estimate the binding affinity of ligands in receptor complexes. *J. Comput. -Aided Mol. Des.* **1997**, *11*, 425–445.
(20) Verdonk, M. L.; Cole, J. C.; Hartshorn, M. J.; Murray, C. W.; Taylor, R. D. Improved protein–ligand docking using GOLD. *Proteins* **2003**, *52*, 609–623.
(21) Korb, O.; Stützle, T.; Exner, T. E. Empirical scoring functions for advanced protein–ligand docking with PLANTS. *J. Chem. Inf. Model.* **2009**, *49*, 84–96.
(22) Hong, L.; Koelsch, G.; Lin, X.; Wu, S.; Terzyan, S.; Ghosh, A. K.; Zhang, X. C.; Tang, J. Structure of the protease domain of memapsin 2 (β-secretase) complexed with inhibitor. *Science* **2000**, *290*, 150–153.

(23) Wang, Y.-S.; Strickland, C.; Voigt, J. H.; Kennedy, M. E.; Beyer, B. M.; Senior, M. M.; Smith, E. M.; Nechuta, T. L.; Madison, V. S.; Czarniecki, M.; McKittrick, B. A.; Stamford, A. W.; Parker, E. M.; Hunter, J. C.; Greenlee, W. J.; Wyss, D. F. Application of fragment-based NMR screening, X-ray crystallography, structure-based design, and focused chemical library design to identify novel ~~μ~~μM~~M~~ leads for the development of nM BACE-1 (β-site APP cleaving enzyme 1) inhibitors. *J. Med. Chem.* **2010**, *53*, 942–950.
(24) Patel, S.; Vuillard, L.; Cleasby, A.; Murray, C. W.; Yon, J. Apo and inhibitor complex structures of BACE (β-secretase). *J. Mol. Biol.* **2004**, *343*, 407–416.
(25) ~~Discovery~~*Discovery Studio* ~~Studio,~~ versions 2.1 and 2.5~~.~~; Accelrys Inc.~~,~~; San Diego, CA .
(26) Rydberg, E. H.; Brumshtein, B.; Greenblatt, H. M.; Wong, D. M.; Shaya, D.; Williams, L. D.; Carlier, P. R.; Pang, Y.-P.; Silman, I.; Sussman, J. L. Complexes of alkylene-linked tacrine dimers with *Torpedo californica* ~~Torpedo californica~~ acetylcholinesterase: ~~binding~~Binding of bis(5)-tacrine produces a dramatic rearrangement in the active-site gorge. *J. Med. Chem.* **2006**, *49*, 5491–5500.
(27) (a) Convertino, M.; Vitalis, A.; Caflisch, A. Disordered binding of small molecules to ~~A~~Aβ*β* (12~~–~~–28). *J. Biol. Chem.* **2011**, *286*, 41578–41588. (b) Scherzer-Attali, R.; Pellarin, R.; Convertino, M.; Frydman-Marom, A.; Egoz-Matia, N.; Peled, S.; Levy-Sakin, M.; Shalev, D. E.; Caflisch, A.; Gazit, E.; Segal, D. Complete phenotypic recovery of an ~~Alzheimer's~~Alzheimer's disease model by a quinone~~–~~–tryptophan hybrid aggregation inhibitor. *PLoS ~~ONE~~One* **2010**, *5*, ~~e11101~~e11101. (c) Scherzer-Attali, R.; Convertino, M.; Pellarin, R.; Gazit, E.; Segal, D.; Caflisch, A. Methylations of tryptophan-modified naphthoquinone affect its inhibitory potential toward ~~A~~Aβ*β* aggregation. *J. Phys. Chem. B* **2013**, *117*, 1780–1789.
(28) Lemkul, J. A.; Bevan, D. R. The role of molecular simulations in the development of inhibitors of amyloid β-peptide aggregation for the treatment of Alzheimer's disease. *ACS Chem. Neurosci.* **2012**, *3*, 845–856.
(29) Lührs, T.; Ritter, C.; Adrian, M.; Riek-Loher, D.; Bohrmann, B.; Döbeli, H.; Schubert, D.; Riek, R. 3D structure of Alzheimer's amyloid-β(1~~–~~–42) fibrils. *Proc. Natl. Acad. Sci. U.S.A.* **2005**, *102*, 17342–17347.
(30) Brooks, B. R.; Bruccoleri, R. E.; Olafson, B. D.; States, D. J.; Swaminathan, S.; Karplus, M. CHARMM: ~~a~~A program for macromolecular energy, minimization, and dynamics calculations. *J. Comput. Chem.* **1983**, *4*, 187–217.
(31) Haberthür, U.; Caflisch, A. FACTS: ~~fast~~Fast analytical continuum treatment of solvation. *J. Comput. Chem.* **2008**, *29*, 701–715.
(32) Domínguez, J. L.; Villaverde, M. C.; Sussman, F. Effect of pH and ligand charge state on BACE-1 fragment docking performance. *J. Comput .-Aided Mol. Des.* **2013**, *27*, 403–417.
(33) Asso, V.; Ghilardi, E.; Bertini, S.; Digiacomo, M.; Granchi, C.; Minutolo, F.; Rapposelli, S.; Bortolato, A.; Moro, S.; Macchia, M. α-Naphthylaminopropan-2-ol derivatives as BACE1 inhibitors. ~~*Chem. Med. Chem.*~~*ChemMedChem* **2008**, *3*, 1530–1534.
(34) Paleo, M. R.; Aurrecoechea, N.; Jung, K.-Y.; Rapoport, H. Formal enantiospecific synthesis of (+)-FR900482. *J. Org. Chem.* **2003**, *68*, 130–138.
(35) Convertino, M.; Pellarin, R.; Catto, M.; Carotti, A.; Caflisch, A. 9,10-Anthraquinone hinders β-aggregation: How does a small molecule interfere with Aβ-peptide amyloid fibrillation?. *Protein Sci.* **2009**, *18*, 792–800.
(36) Nicolet, Y.; Lockridge, O.; Masson, P.; Fontecilla-Camps, J. C.; Nachon, F. Crystal structure of human butyrylcholinesterase and of its complexes with substrate and products. *J. Biol. Chem.* **2003**, *278*, 41141–41147.
(37) Koes, D. R.; Camacho, C. J. ZINCPharmer: ~~pharmacophore~~Pharmacophore search of the ZINC database. *Nucleic Acids Res.* **2012**, *40*, W409–W414.
(38) Li, S.-Y.; Jiang, N.; Xie, S.-S.; Wang, K. D. G.; Wang, X.-B~~.~~.; Kong, L.-Y. Design, synthesis and evaluation of novel tacrine~~–~~–rhein hybrids as multifunctional agents for the treatment of Alzheimer's disease. *Org. Biomol. Chem.* **2014**, *12*, 801–814.
(39) Wang, Y.; Xia, Z.; Xu, J.-R.; Wang, Y.-X.; Hou, L.-N.; Qiu, Y.; Chen, H.-Z. α-Mangostin, a polyphenolic xanthone derivative from mangosteen, attenuates β-amyloid oligomers-induced neurotoxicity by inhibiting amyloid aggregation. *Neuropharmacology* **2012**, *62*, 871–881.
(40) Buchanan, L. E.; Dunkelberger, E. B.; Tran, H. Q.; Cheng, P.-N.; Chiu, C.-C.; Cao, P.; Raleigh, D. P.; de Pablo, J. J.; Nowick, J. S.; Zanni, M. T. Mechanism of IAPP amyloid fibril formation involves an intermediate with a transient β-sheet. *Proc. Natl. Acad. Sci. U.S.A.* **2013**, *110*, 19285–19290.
(41) Ahmed, M.; Davis, J.; Aucoin, D.; Sato, T.; Ahuja, S.; Aimoto, S.; Elliot, J. I.; Van Nostrand, W. E.; Smith, S. O. Structural conversion of neurotoxic amyloid-$\beta_{1-42}$ oligomers to fibrils. *Nat. Struct. Mol. Biol.* **2010**, *17*, 561–567.